



New zircon U-Pb LA-ICP-MS ages and Hf isotope data from the Central Pontides (Turkey): Geological and geodynamic constraints

Okay Çimen^{a,b,*}, M. Cemal Göncüoğlu^b, Antonio Simonetti^c, Kaan Sayit^b

^a Munzur University, Department of Geological Engineering, 62000 Tunceli, Turkey

^b Middle East Technical University, Department of Geological Engineering, 06800 Ankara, Turkey

^c University of Notre Dame, Department of Civil and Environmental Engineering and Earth Sciences, South Bend, IN 46556, USA



ARTICLE INFO

Keywords:

Intra-Pontide ocean
Jurassic
Arc magmatism
Central Pontides
N Turkey

ABSTRACT

The Central Pontides in northern Anatolia is located on the accretionary complex formed by the closure of Neotethyan Intra-Pontide Ocean between the southern Eurasian margin (Istanbul-Zonguldak Terrane) and the Cimmerian Sakarya Composite Terrane. Among other components of the oceanic lithosphere, it comprises not yet well-dated felsic igneous rocks formed in arc-basin as well as continent margin settings. In-situ U-Pb age results for zircons from the arc-basin system (Çangaldağ Metamorphic Complex) and the continental arc (Devrekani Metadiorite and Granitoid) yield ages of 176 ± 6 Ma, 163 ± 9 Ma and 165 ± 3 Ma, respectively. Corresponding in-situ average (initial) $^{176}\text{Hf}/^{177}\text{Hf}$ initial ratios are 0.28261 ± 0.00003 , 0.28267 ± 0.00002 and 0.28290 ± 0.00004 for these units and indicative of a subduction-modified mantle source. The new U-Pb ages and Hf isotope data from these oceanic and continental arc units together with regional geological constraints support the presence of a multiple subduction system within the Intra-Pontide Ocean during the Middle Jurassic.

1. Introduction

The closure of the Tethyan oceanic branches along the Alpine-Himalayan orogenic belt resulted in accretion of a number of oceanic and continental micro-plates (e.g. Sengör and Yilmaz, 1981) or terranes (e.g. Göncüoğlu et al., 1997; Okay and Tuysuz, 1999; Stampfli and Borel, 2002). In the Eastern Mediterranean and especially in Anatolia, the sutures of these oceanic branches existing during the mid-Mesozoic are known as the Neotethyan suture belts (e.g. Göncüoğlu, 2010). From these (Fig. 1), the southernmost (the Bitlis-Zagros Suture) and the middle (the Izmir-Ankara-Erzincan-Sevan-Akera Suture) are relatively well-studied (for a brief review see Robertson et al., 2013). However, the tectonic and geodynamic history of northernmost suture, the Intra-Pontide Suture (IPS), is still a matter of debate. It was initially suggested by Sengör and Yilmaz (1981) that the IPS is bound to the north by the Rhodope-Pontide fragment and by the Sakarya Continent to the south. However, the location, opening and closure ages, subduction polarity, even the existence of the corresponding oceanic branch (the Neotethyan Intra-Pontide Ocean (IPO)) is still disputed (e.g., Robertson and Ustaömer, 2004). Recent field studies in the central part of the IPS, supported by new and precise radiometric age data (Okay et al., 2014; Çimen, 2016) indicate that the IPS formed by the closure of the IPO during the Mid-Late Mesozoic resulting from N-ward subduction and

stepwise accretion of oceanic/continent margin assemblages to the Eurasian margin (e.g. Okay et al., 2006; Göncüoğlu et al., 2014; Sayit et al., 2016; Çimen et al., 2016, 2017). In the Central Pontides (CP), the very thick structural complex comprising mainly oceanic assemblages is referred to as the Central Pontide Structural Complex (CPSC; Tekin et al., 2012). It is mainly represented by variably metamorphosed supra-subduction type basic volcanic rocks and associated sediments. A comparatively less-voluminous member of the IPS is characterized by felsic, intermediate and mafic extrusive and intrusive rocks (e.g. Ustaömer and Robertson, 1999; Okay et al., 2013; Çimen et al., 2016), of island-arc (Çangaldağ Metamorphic Complex), and continental arc (Çangaldağ Pluton; Çimen et al., 2017) origins. In contrast to the oceanic basalts, the tectono-magmatic evolutions as well as the ages of these arc-assemblages have yet to be studied in detail. Moreover, distinct arc-type magmatism of Jurassic age is reported (McCann et al., 2010; Meijers et al., 2010; Dokuz et al., 2017) from the neighbouring terranes such as the Eastern Pontides, Crimea and Greater Caucasus (Figs. 1 and 2). However, a reliable correlation of the age and tectono-magmatic setting of this arc-type magmatism with the rock assemblages present within the CP is hampered by the scarcity of radiometric age data.

In this paper, new radiometric age and Hf isotope data are reported from the widespread oceanic arc (Çangaldağ Metamorphic Complex; a

* Corresponding author at: Munzur University, Department of Geological Engineering, 62000 Tunceli, Turkey.

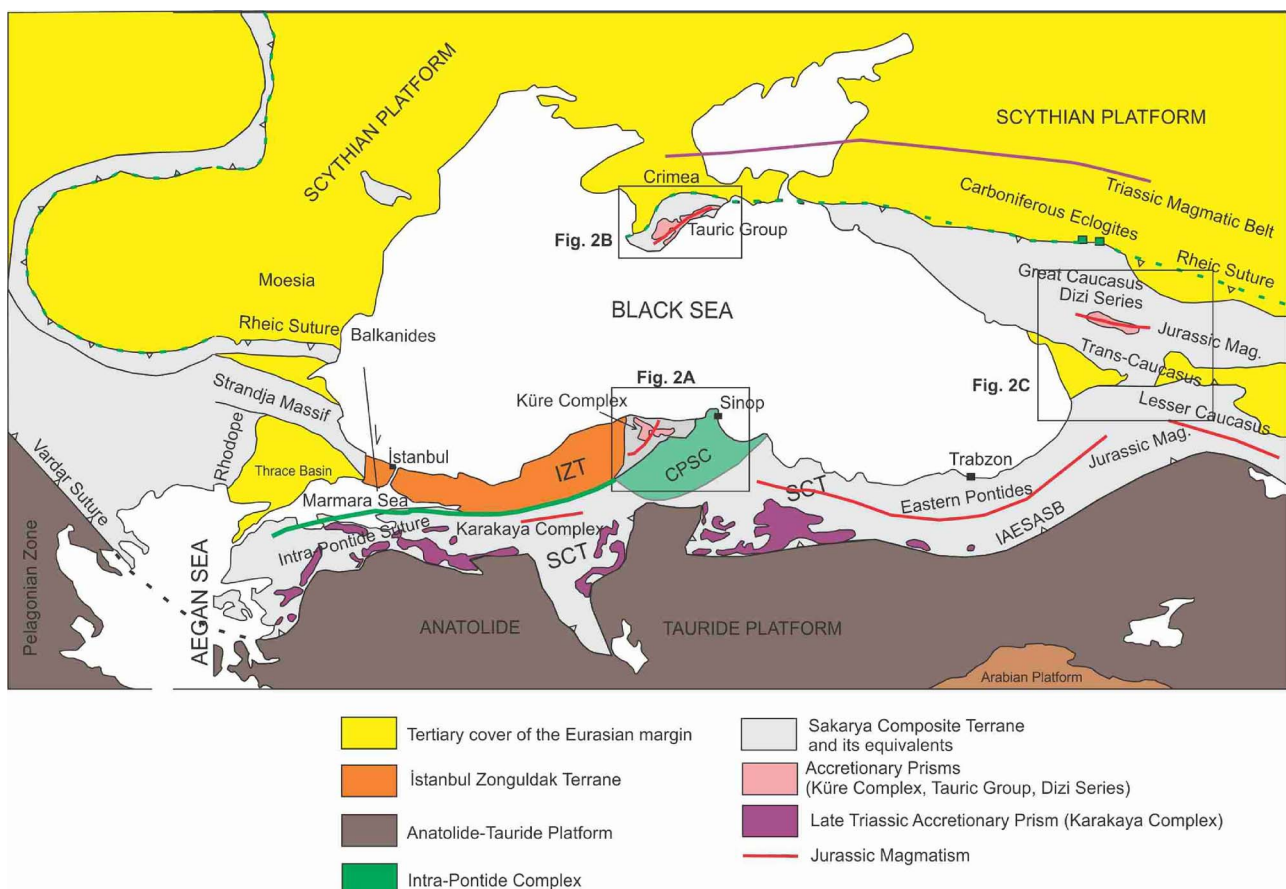


Fig 1. Tectonic map of the Black Sea region with the main alpine terranes (modified from Okay and Nikishin, 2015; Çimen et al., 2017); CPSC: Central Pontide Structural Complex. SCT: Sakarya Composite Terrane. IZT: İstanbul-Zonguldak Terrane. IAESASB: İzmir-Ankara-Erzincan-Sevan-Akera Suture Belt.

part of the CPSC) and continental margin (Devrekani Granitoid and Metadiorite) magmatism in the CP. The aim is to provide useful inferences and insights into the geological evolution of the CP and the Black Sea region during the Middle Jurassic.

2. Geological framework

The “Central Pontides” is a geographical term comprising several units with geographical (e.g. Devrekani Massif, Kargı Massif, Daday Massif, Ilgaz Massif) or tectonic (e.g. Küre Complex, Gemic Complex, Devrekani Metamorphics, CMC, Elekdağ Complex, Domuzdağ-Saraycık Complex) origin (Yılmaz and Tuysuz, 1984; Ustaömer and Robertson, 1999; Kozur et al., 2000; Göncüoğlu et al., 2012, 2014; Okay et al., 2006, 2013, 2014, 2015; Okay and Nikishin, 2015; Aygül et al., 2016; Sayit et al., 2016; Çimen et al., 2016; Gücer et al., 2016) (Fig. 2a). It includes the tectonic boundary between the Gondwana-derived İstanbul-Zonguldak Terrane (IZT) in the N, the Cimmerian Sakarya Composite Terrane (SCT) in the S and remnants of the Neotethyan IPS Belt (Figs. 1, 2a) between them (e.g. Göncüoğlu, 2010). The large area of metamorphic rocks in the southern part of the CP, previously interpreted as the remnant of Paleotethys (e.g. Göncüoğlu et al., 1997; Okay and Tuysuz, 1999) has been recently proven to be Mid-Jurassic-Cretaceous in age (e.g. Okay et al., 2006), and defined as the CPSC (Tekin et al., 2012; Frassi et al., 2016; Çimen et al., 2016) of the IPS. It comprises the Daday Massif in the west, the Elekdağ-Domuzdağ and Kargı massifs in the east, and the Çangaldağ Metamorphic Complex (CMC) in the north (Fig. 2a). The CMC is bounded in the north by the Çangaldağ Pluton that intrudes the southern Eurasian continental margin.

2.1. Pre-middle Jurassic structural units of the Eurasian margin

The Paleozoic Terranes of the Eurasian margin are represented by the Devrekani Metamorphics and Gemic Complex (Okay et al., 2015; Gücer et al., 2016), and Permo-Carboniferous Sivrikaya and Deliktaş Granitoids (Nzegge, 2008) in the CP (Fig. 2a, d).

2.1.1. Gemic Complex, Sivrikaya and Deliktaş granitoids

The Gemic Complex has been recently studied by Okay et al. (2014). The complex comprises gneisses and migmatites with minor amphibolite and marble. It is intruded by the Middle Jurassic (163 Ma ± 4 Ma) Dikmen Porphyry and unconformably overlain by Lower Cretaceous sandstone and shale (Fig. 2a). The cross-cutting relations indicate a pre-Callovian metamorphic age for the complex. Okay et al. (2014) suggests that the Gemic Complex represents the remobilized basement of the CP.

The Late Carboniferous Sivrikaya (300 ± 1 Ma) and the Early Permian Deliktaş (295 ± 1 Ma) granitoids (Fig. 2a) have been studied by Nzegge (2008). The Sivrikaya granitoid is composed of granodiorites, tonalites and two-mica granites, generated by mixing of partially melted lower continental crust and subcrustal lithospheric mantle. The Deliktaş pluton includes only muscovite-rich monzogranites displaying geochemical characteristics of S-type granites. Both granitoids have been interpreted as magmatic products of orogenic collisional tectonics, and crustal thickening during northward subduction of a Paleozoic ocean (the Paleotethys Ocean in Nzegge, 2008).

2.1.2. Devrekani Metamorphics

The Devrekani Metamorphics terrane is structurally located between the Küre Complex and the CMC (Figs. 2 and 3). It comprises medium-to high-grade metamorphic rocks including paragneiss,

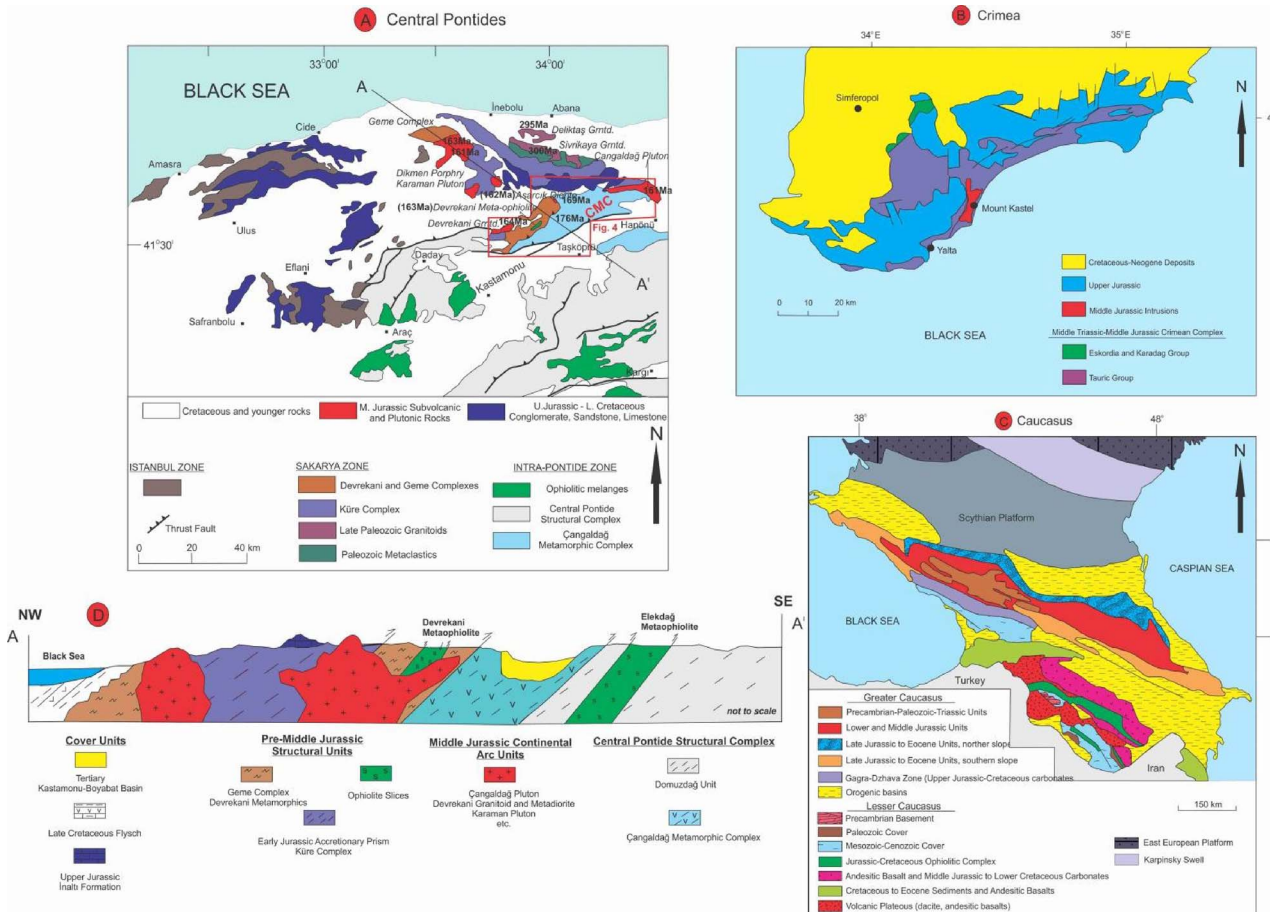


Fig. 2. Geological maps of the (A) Central Pontides (modified after Okay et al., 2015; Göncüoğlu et al., 2012, 2014; Ustaömer and Robertson, 1999; Çimen et al., 2017). CMC: Çangaldag Metamorphic Complex. Grndt: Granitoid. Age data taken from Nzege (2008); Okay et al. (2014); Çimen (2016); Çimen et al. (2017) and this study (B) Crimea (modified from Solov'ev and Rogov, 2010 and (C) Caucasus (McCann et al., 2010) regions (D) Sketch cross section of the main tectonic units in the Central Pontides (modified from Ustaömer and Robertson, 1999; Çimen, 2016; Çimen et al., 2017).

amphibolite and marbles, which have been metamorphosed to amphibolite and granulite facies conditions (Boztuğ and Yılmaz, 1995; Boztuğ et al., 1995; Ustaömer and Robertson, 1999). The unit is intruded by variably deformed and metamorphosed granitoids (Fig. 4a), which are referred to as “orthogneisses” in this study. The presence of such meta-granitoids is a common feature of different Variscan basements (Göncüoğlu, 2010) in northern Turkey.

The protoliths of the amphibolites, orthogneisses and paragneisses have been interpreted as island-arc tholeiitic basalts, I-type calc-alkaline volcanic arc granitoids and clastic sediments (shale-wackestone), respectively (Güçer et al., 2016). The Devrekani Metamorphics have been evaluated as the products of Permo-Carboniferous (316 ± 9 Ma– 252 ± 9 Ma) arc affected by Jurassic metamorphism (Güçer et al., 2016). Yılmaz and Bonhomme (1991) reported an age of metamorphism for the Devrekani Metamorphics of 149 ± 4 Ma to 170 ± 10 Ma on the basis of K-Ar mica and amphibole ages. Recently, similar Jurassic Ar-Ar mica ages of 151 ± 1 Ma and 156 ± 2 Ma were reported by Okay et al. (2014) and Güçer et al. (2016), respectively.

Moreover, metaophiolite slices (Dibekdere metaophiolite of Yılmaz, 1980) are tectonically intercalated within the Devrekani Metamorphics (Fig. 3) and sandwiched between the Devrekani Metamorphics and the CMC. The metaophiolite slice within the Devrekani Metamorphics in the studied area is about 3.5 km thick and stretches for more than 15 kms in NE-SW direction (Fig. 3). It mainly comprises harzburgites and dunites with chromite veins. The other metaophiolite slice between the Devrekani and CMC is located in the SW corner of the study area (Fig. 3). The slice is more than 2 km thick and mainly includes highly deformed cumulate metagabbros, plagiogranites, dolerites and

metabasalts adjacent to serpentinites. The formation age of these metaophiolites as well as the age of their imbrication with the Devrekani Metamorphics is unknown, and to date there are no published radiometric age data. In the former slice, two metadiorite bodies were observed to cross-cut the metaophiolite body in different locations (Fig. 4b). The metadiorites display holocrystalline/porphyritic texture and include plagioclase, amphibole, biotite, chlorite and quartz as phenocrysts.

2.2. Middle Jurassic continental arc magmatics at the Eurasian margin

The Middle Jurassic magmatism is represented by several intrusive bodies in the CP (e.g. Devrekani Granitoid, Asarcık Diorite, Dikmen Porphyry, Karaman and Çangaldag Plutons; Fig. 2a). This widespread magmatism (e.g. Çangaldag and Karaman Plutons) cuts the Paleozoic basement units and the Küre Complex at several locations. All of these assemblages are unconformably overlain by cover units such as the Late Jurassic İnalı, Early Cretaceous Çağlayan and Tertiary Units, respectively.

2.2.1. Asarcık Diorite, Karaman Pluton and Dikmen Porphyry

The Asarcık diorite (Fig. 2a) intrudes the Devrekani Metamorphics and the first radiometric age data are reported as Middle Jurassic age (176 ± 7 Ma and 162 ± 5 Ma) with the K-Ar method (Bonhomme and Yılmaz, 1984; Yılmaz and Bonhomme, 1991). Recently, the radiometric age and geological data from the Karaman Pluton and the Dikmen Porphyry have been published by Okay et al. (2014). According to this study, the Karaman Pluton intrudes the Triassic Küre Complex and is

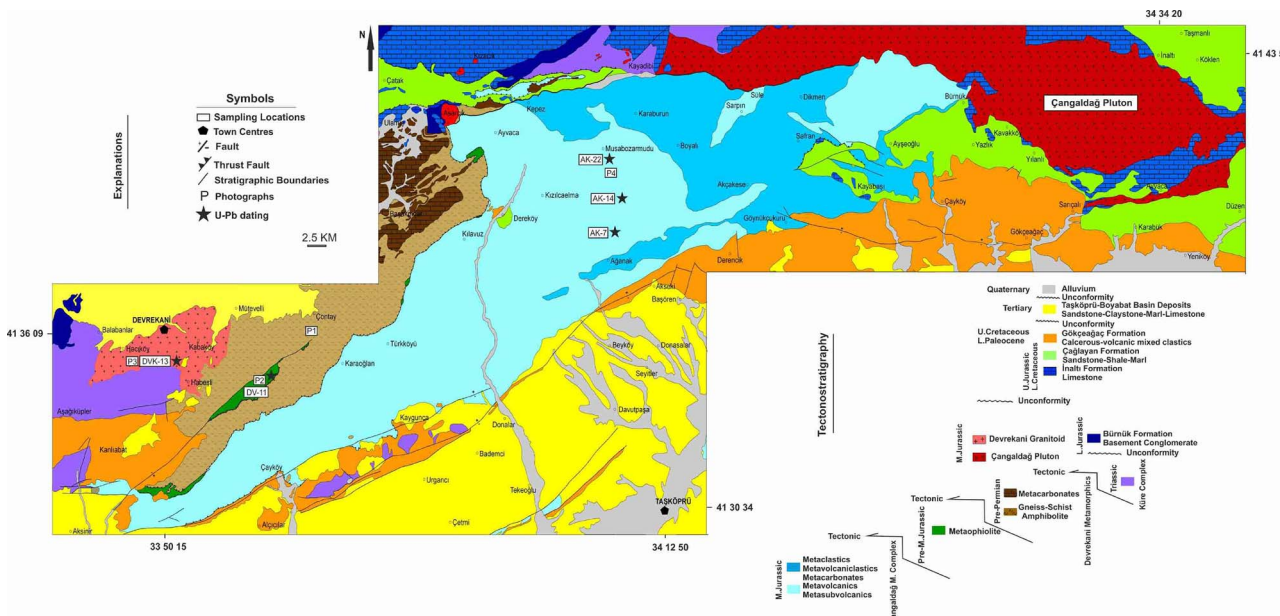


Fig. 3. Geological map of the study area with the sample locations (modified from Konya et al., 1988; Çimen et al., 2017).

Sampling Coordinates: AK-7 = 413948N, 340907E; AK-14 = 414022N, 340949E; AK-22 = 414104N, 340956E; DV-11 = 443455N, 335516E; DVK-13 = 413518N, 335049E

unconformably overlain by the Early Cretaceous turbidites (Fig. 2a). It displays a zoned structure with a core of medium-grained micro-granodiorite to micro-diorite surrounded by dacite porphyry. The Ar–Ar dating of biotite from a dacite–porphyry sample yields a Middle Jurassic age (162 ± 4 Ma, Okay et al., 2014).

The Dikmen Porphyry intrudes the Geme Complex and is unconformably overlain by the Lower Cretaceous turbidites (Fig. 2a). It is a shallow-level intrusion and composed of porphyritic grey andesite and dacite. Ar–Ar dating of biotite from one dacite porphyry sample yields a Middle Jurassic age as well ($163 \text{ Ma} \pm 4 \text{ Ma}$; Okay et al.,

2014). Another Late Jurassic ($160.5 \text{ Ma} \pm 1.2 \text{ Ma}$) whole rock Ar–Ar data is reported from “basic dikes” cross-cutting the Devrekani Metamorphics, and interpreted as a cooling age, reset by the intrusion of Middle Jurassic granitoids (Sarifakioğlu et al., 2017).

2.2.2. Çangaldağ Pluton

Three different rock groups, gabbroic diorite, dacite porphyry and granite, were noted within the Çangaldağ Pluton. This intrusive body intrudes the Triassic Küre Complex in the east and is overlain by the İnaltı Formation (Fig. 3). There is an oblique fault between the

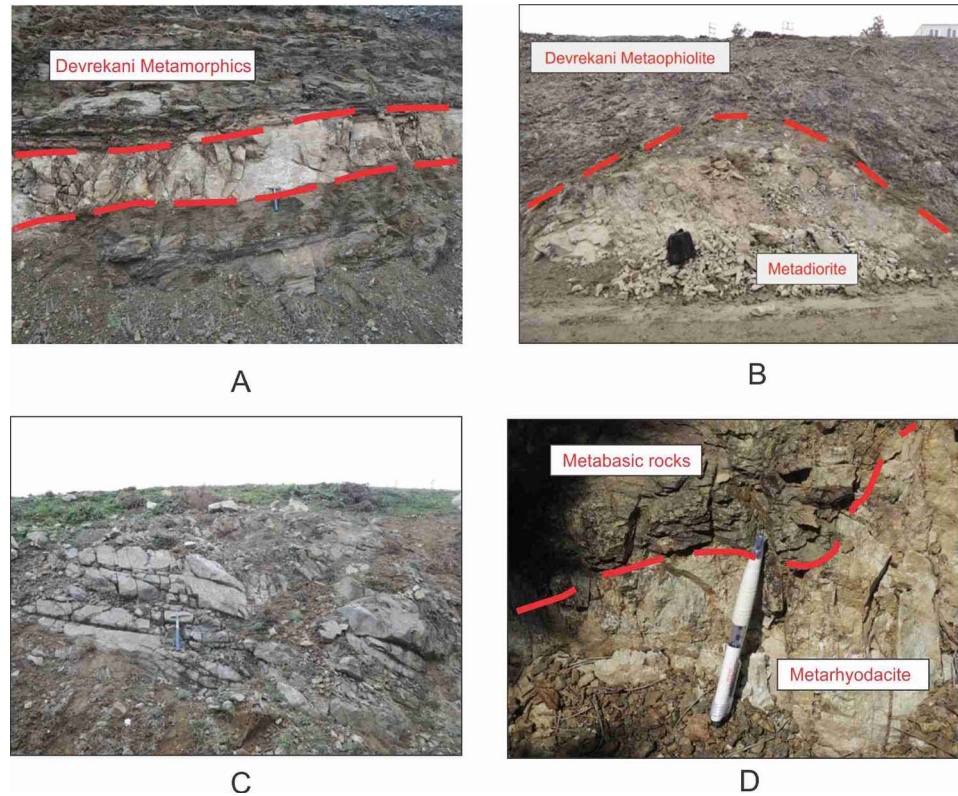


Fig. 4. (A) An image of the cross-cutting relation between the Devrekani Orthogneiss and the Devrekani Metamorphics (Locality P1). (B) An image of the cross-cutting relation between the Devrekani Metadiorite and the Devrekani Metaophiolite (Locality P2). (C) Field image of the granite body within the Devrekani Granitoid (Locality P3). (D) An image of the cross-cutting relation between the metabasic rocks and metarhyodacites within the CMC (Locality P4).

Çangaldağ Pluton and the CMC units according to field observations. Based upon the cross-cutting relation between the Çangaldağ Pluton and the Küre Complex, its age must be between Triassic and Late Jurassic; this observation was recently confirmed by in-situ U-Pb zircon ages of Middle Jurassic (161 ± 5 Ma and 170 ± 2 Ma; Çimen et al., 2017). Overall, the geological and petrological data reported by Çimen et al. (2017) indicate that the CP represents a Middle Jurassic arc system, and propose that the Çangaldağ Pluton formed within a continental arc during northward subduction of the IPO.

2.2.3. Devrekani Granitoid

The Devrekani Granitoid outcrops to the south Devrekani town of Kastamonu (Figs. 2a, 3) and is mainly composed of diorites and granites (Fig. 4c). Additionally, Nzegge (2008) has geochemically identified the presence of tonalite bodies within this unit. They are characterized by a medium grain size and whitish/greenish color. The igneous body has been affected by intense alteration processes and it is therefore difficult to differentiate the rock types in the field. Geologically, the Devrekani Granitoid cuts the Triassic Küre Complex in the south and the Devrekani Metamorphics to the east of Devrekani. It is disconformably covered by the Tertiary units in the north (Fig. 3). The geochemical systematics of the Devrekani Granitoid shows the typical characteristics of subduction-related magmatism (Nzegge, 2008). Also, the age of the unit was dated as Middle Jurassic (from 170 ± 2 Ma to 165 ± 5 Ma) using single zircon evaporation method (Nzegge, 2008). In this study, one granite sample (DVK-13) was taken from the Devrekani Granitoid for geochronological investigation. It displays porphyritic texture and contains plagioclase, K-feldspar and quartz phenocrysts embedded in a medium-grained groundmass that includes biotite, chlorite and amphibole. Here, we present new radiometric age data for this unit using an in-situ LA-ICP-MS U-Pb dating method.

2.3. Early Jurassic island arc of the IPS

The oceanic assemblages of the IPS are included in the CPSC (Figs. 1, 2a,d) consisting of several tectonic units such as the CMC, Domuzdağ Unit, Emirköy Unit, Aylı Dağ Unit, Arkot Dağ Unit, Saka Unit and Daday Unit (for details see Sayit et al., 2016 and Frassi et al., 2016, 2018). From these the northerly located (Fig. 2a) CMC is the only unit with felsic to intermediate rocks representing an island arc within the IPO. All others outcrop in the southern part of the CPSC and include a structural pile of supra-subduction type metabasic rocks (e.g. Ustaömer and Robertson, 1999; Okay et al., 2006, 2013, Göncüoğlu et al., 2012, 2014; Tekin et al., 2012; Marroni et al., 2014; Sayit et al., 2016; Frassi et al., 2016).

2.3.1. Çangaldağ Metamorphic Complex

The CMC is tectonically bounded by the Devrekani Metamorphics in the north and the Taşköprü-Boyabat Tertiary basin to the south (Figs. 2a, d, 3). Initially, the CMC had been defined as a metaophiolitic body by several authors (Yılmaz, 1980, 1983; Yılmaz and Tüysüz, 1984; Şengün et al., 1988; Tüysüz, 1985, 1990; Boztuğ and Yılmaz, 1995). Later, it was ascribed to a structurally thickened pile of mainly volcanic rocks and subordinate volcanioclastic rocks that overlie a basement of sheeted dykes in the north and basic extrusives in the south (Ustaömer and Robertson, 1999).

According to a recent study (Çimen et al., 2016); the CMC is composed of low-grade metamorphic rocks of intrusive, extrusive, and volcanioclastic origin that exhibit a wide range of felsic to mafic compositions. Petrographically, it consists of basalts-andesites-rhyodacites and tuffs with minor amount of gabbros and diabases. Most of these magmatic rocks are metamorphosed to greenschist facies conditions (Çimen et al., 2016). In the field, the contacts between the main igneous rock bodies are sheared whereas intrusive relations are observed between the metavolcanioclastic/metabasic rocks and the meta-rhyodacites (Fig. 4d). The thickness of these metarhyodacite bodies within the

CMC vary between 3 and 15 m. They display white and slightly brownish colors and mostly porphyritic and microcrystalline textures. The phenocryst phases are characterized by quartz, feldspar and minor biotite in a fine-grained groundmass. Quartz phenocrysts exhibit undulatory extinction and the feldspar minerals mostly have been altered to sericite.

The overall geochemical characteristics of the CMC indicate its derivation from a subduction modified mantle source (Ustaömer and Robertson, 1999; Çimen, 2016). Overall, the CMC was presumably formed in both arc and back-arc regions above an intra-oceanic subduction within the IPO (Çimen et al., 2016). Specifically, the metarhyodacites are variably depleted in Nb compared to LREEs and display geochemical similarities to dacites from oceanic arcs, such as Mariana (Çimen et al., 2016).

Three metarhyodacite samples (AK-7, AK-14 and AK-22) were taken from the CMC from the central part of the study area (Fig. 3) in order to date the intrusion by zircon U-Pb laser ablation-multicollector-inductively coupled plasma mass spectrometry (LA-MC-ICP-MS) method. Previous studies have reported K-Ar ages of Middle Jurassic ($153 \text{ Ma} \pm 16 \text{ Ma}$) and Early Cretaceous metamorphism ($126 \pm 4 \text{ Ma}$ – $110 \pm 5 \text{ Ma}$) for the CMC's metabasic rocks and phyllites, respectively (Yılmaz and Bonhomme, 1991). Early Cretaceous metamorphic ages have been corroborated by Okay et al. (2013) for the complex with more reliable white-mica Ar-Ar age determinations of $136 \pm 4 \text{ Ma}$ and $125 \pm 1 \text{ Ma}$. Moreover, Okay et al. (2014) published a single Middle Jurassic ($169 \pm 2 \text{ Ma}$) U-Pb radiometric age determination for a metadacite sample, which represents the protolith of the CMC.

2.4. Cover units

The sedimentary cover units are grouped as the “first allochthonous cover” comprising the Late Jurassic Bürnük and İnalı formations, the “second allochthonous cover” consisting of the Early Cretaceous Çağlayan and Late Cretaceous/Early Paleocene Gökçeağac formations (Üguz and Sevin, 2007), and the Tertiary cover of the Taşköprü-Boyabat Basin (Fig. 3).

3. Analytical methods

Three metarhyodacite samples (AK-7, AK-14, AK-22) from the CMC, one sample of metadiorite (DV-11) intruding the Devrekani Metaophiolite, and one granite sample from the Devrekani Granitoid (DVK-13) were examined for U-Pb age determinations. The detailed sample preparation process including heavy mineral separation and hand-picking of crystals using a petrographic microscope are reported in Çimen et al. (2017). In total, ~60 zircon grains were embedded on a glass slide and polished in order to observe their internal structures. The zircons were imaged by cathodoluminescence using a Cameca SX50 electron microprobe instrument before LA-MC-ICP-MS analysis (Figs. 5 and 6). In order to validate the accuracy of the U-Pb age results reported here (Tables 1–3), three well established zircon standards, Plešovice (Slama et al., 2008), 91500 (Wiedenbeck et al., 1995), and GJ-1 (Jackson et al., 2004) were also analysed throughout the analytical sessions. The detailed analytical procedure is included in the Appendix file.

In situ Hf isotope measurements were conducted on the same zircon grains investigated for U-Pb age determinations. As used for the in-situ U-Pb analyses, the same LA-MC-ICP-MS instrument configuration was employed for the in-situ Hf analyses. Three well characterized zircon standards for their Hf isotope compositions, Plešovice (Slama et al., 2008), 91500 (Woodhead and Hergt, 2005), and BR266 (Woodhead et al., 2004) were analyzed at the start of each analytical session in order to ensure the accuracy of the in-situ Hf results reported here (Tables 4–6). The detailed analytical procedure is included in the Appendix file.

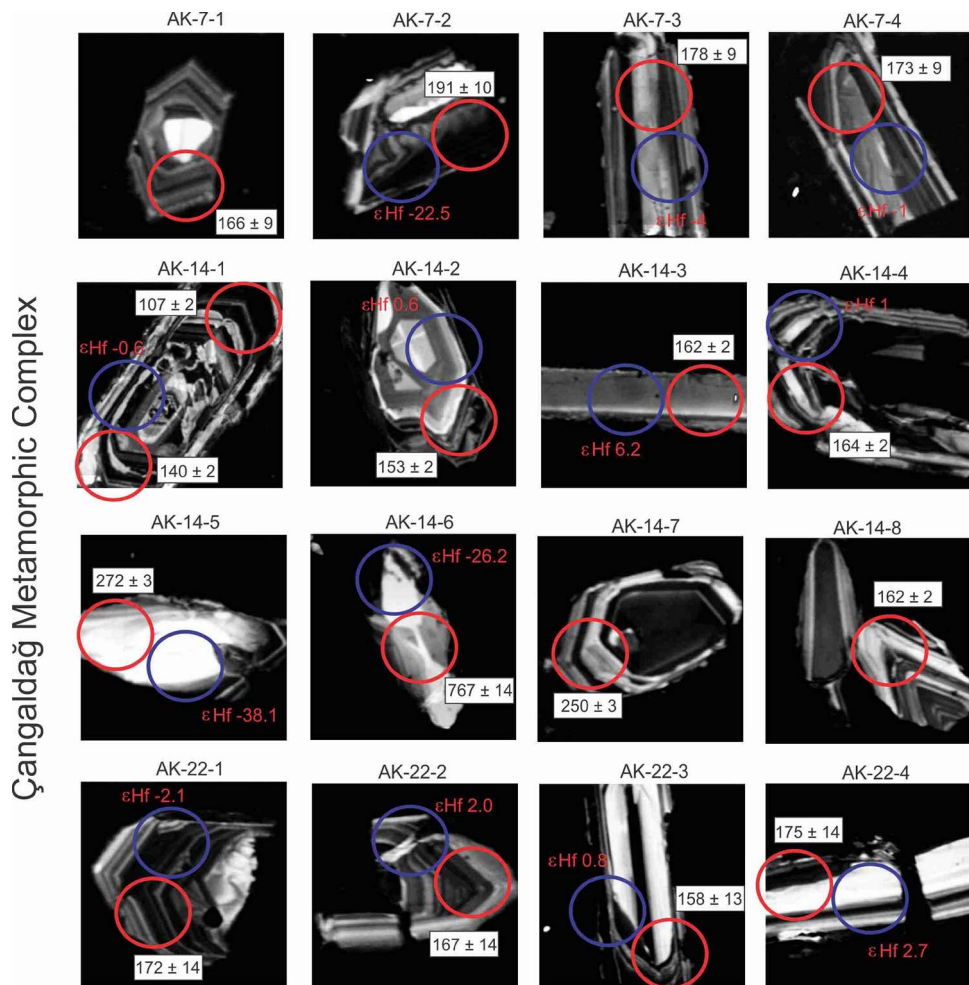


Fig. 5. CL images of zircon grains from Çangaldağ Metamorphic Complex samples AK-7, AK-14 and AK-22 (Red circles: U-Pb ($^{207}\text{Pb}/^{235}\text{U}$) spots-35 μm , Blue circles: Hf spots-35 μm). (For interpretation of the references to colour in this figure legend, the reader is referred to the web version of this article.)

4. Results and discussion

4.1. U-Pb geochronology

4.1.1. Çangaldağ Metamorphic Complex

The U-Pb zircon geochronometer is amongst the most reliable

radiometric methods for determining the age of igneous rocks (e.g., Simonetti et al., 2005). Zircon grains ($n = 16$) from three metarhyodacite samples (AK-7, AK-14 and AK-22) within the CMC were analyzed and the U-Pb age results are reported in Table 1. The morphology of the analyzed zircons ranges from rounded to euhedral in shape, and internal structures may be diffused, oscillatory, laminated and unzoned

Table 1

U-Pb isotopic data for zircons in the metarhyodacite samples from the Çangaldağ Metamorphic Complex.

Grain #	^{238}U (volts)	^{206}Pb (cps)	$^{206}\text{Pb}/^{204}\text{Pb}$	$^{206}\text{Pb}/^{238}\text{U}$	2σ	$^{207}\text{Pb}/^{235}\text{U}$	2σ	$^{207}\text{Pb}/^{206}\text{Pb}$	2σ	$^{206}\text{Pb}/^{238}\text{U}$ Age (Ma)	$^{207}\text{Pb}/^{235}\text{U}$ Age (Ma)	$^{207}\text{Pb}/^{206}\text{Pb}$ Age (Ma)
AK-7-1	0.5110	578125	40000	0.0262	0.0013	0.2100	0.0105	0.0581	0.0029	166 ± 9	193 ± 10	533 ± 27
AK-7-2	0.4680	573125	31000	0.0301	0.0015	0.2680	0.0134	0.0635	0.0032	191 ± 10	239 ± 12	693 ± 35
AK-7-3	0.4090	486250	36200	0.0280	0.0014	0.2220	0.0111	0.0575	0.0029	178 ± 9	203 ± 11	506 ± 26
AK-7-4	0.2309	270313	0.0000	0.0273	0.0014	0.1932	0.0097	0.0517	0.0026	173 ± 9	179 ± 9	270 ± 14
AK-14-1-1	0.1510	113750	16470	0.0169	0.0003	0.3867	0.0062	0.1692	0.0020	107 ± 2	331 ± 5	2544 ± 20
AK-14-1-2	0.1772	171250	480	0.0220	0.0003	0.3653	0.0057	0.1195	0.0009	140 ± 2	315 ± 5	1946 ± 13
AK-14-2	0.0718	80313	26000	0.0241	0.0003	0.2030	0.0022	0.0612	0.0007	153 ± 2	187 ± 2	641 ± 23
AK-14-3	0.2821	316813	30000	0.0256	0.0003	0.1854	0.0018	0.0527	0.0003	162 ± 2	172 ± 2	315 ± 13
AK-14-4	0.4100	461250	69700	0.0258	0.0003	0.2164	0.0015	0.0607	0.0005	164 ± 2	198 ± 2	626 ± 16
AK-14-5	0.1097	220000	11770	0.0431	0.0004	0.7940	0.0130	0.1340	0.0018	272 ± 3	592 ± 8	2145 ± 24
AK-14-6	0.0924	520625	infinite	0.1260	0.0025	2.0840	0.0430	0.1196	0.0006	767 ± 14	1144 ± 14	1949 ± 9
AK-14-7	0.2570	451875	18450	0.0397	0.0005	0.4288	0.0047	0.0789	0.0007	250 ± 3	362 ± 4	1164 ± 18
AK-14-8	0.3559	398750	21000	0.0256	0.0002	0.1870	0.0012	0.0530	0.0003	162 ± 2	174 ± 2	329 ± 11
AK-22-1	0.5932	697500	10460	0.0271	0.0022	0.3084	0.0247	0.0826	0.0066	172 ± 14	272 ± 22	1257 ± 100
AK-22-2	0.3790	436250	15000	0.0263	0.0021	0.2279	0.0182	0.0628	0.0050	167 ± 14	208 ± 17	686 ± 54
AK-22-3	0.4040	438125	20500	0.0248	0.0020	0.2344	0.0188	0.0685	0.0055	158 ± 13	213 ± 18	878 ± 70
AK-22-4	0.1115	140188	41000	0.0276	0.0022	0.2393	0.0191	0.0628	0.0050	175 ± 14	217 ± 18	680 ± 54

Table 2

U-Pb isotopic data for zircons in the Devrekani metadiorite.

Grain #	^{238}U (volts)	^{206}Pb (cps)	$^{206}\text{Pb}/^{204}\text{Pb}$	$^{206}\text{Pb}/^{238}\text{U}$	2σ	$^{207}\text{Pb}/^{235}\text{U}$	2σ	$^{207}\text{Pb}/^{206}\text{Pb}$	2σ	$^{206}\text{Pb}/^{238}\text{U}$ Age (Ma)	$^{207}\text{Pb}/^{235}\text{U}$ Age (Ma)	$^{207}\text{Pb}/^{206}\text{Pb}$ nAge (Ma)
DV-11-1	0.0074	17188	2300	0.0274	0.0005	0.3020	0.0180	0.0799	0.0047	174 ± 4	264 ± 13	1086 ± 94
DV-11-2	0.0610	82813	60000	0.0275	0.0005	0.1979	0.0040	0.0522	0.0016	174 ± 4	183 ± 4	289 ± 69
DV-11-3	0.0302	44188	4400	0.0277	0.0005	0.2200	0.0054	0.0577	0.0020	176 ± 4	201 ± 5	499 ± 69
DV-11-4	0.0946	233750	36000	0.0510	0.0009	0.3743	0.0071	0.0536	0.0016	320 ± 6	322 ± 6	352 ± 68
DV-11-5	0.0626	83188	13000	0.0268	0.0005	0.2010	0.0049	0.0547	0.0019	170 ± 4	185 ± 5	378 ± 71
DV-11-6	0.0695	196875	11340	0.0590	0.0014	0.5083	0.0100	0.0636	0.0021	369 ± 9	417 ± 7	713 ± 71
DV-11-7	0.0813	109563	70000	0.0281	0.0005	0.1992	0.0039	0.0517	0.0016	178 ± 4	184 ± 4	269 ± 68
DV-11-8	0.1442	744375	60000	0.1253	0.0062	1.4670	0.0840	0.0836	0.0026	757 ± 35	893 ± 34	1277 ± 61
DV-11-9	0.2027	465000	12000	0.0496	0.0009	0.3641	0.0069	0.0531	0.0016	312 ± 6	315 ± 6	331 ± 68
DV-11-10	0.0225	35375	infinite	0.0276	0.0006	0.2065	0.0048	0.0540	0.0018	175 ± 4	190 ± 4	360 ± 74
DV-11-11	0.0449	59688	2000	0.0262	0.0005	0.1932	0.0050	0.0537	0.0018	166 ± 4	179 ± 5	348 ± 74

Table 3

U-Pb isotopic data for zircons in the granite sample from the Devrekani Granitoid.

Grain #	^{238}U (volts)	^{206}Pb (cps)	$^{206}\text{Pb}/^{204}\text{Pb}$	$^{206}\text{Pb}/^{238}\text{U}$	2σ	$^{207}\text{Pb}/^{235}\text{U}$	2σ	$^{207}\text{Pb}/^{206}\text{Pb}$	2σ	$^{206}\text{Pb}/^{238}\text{U}$ Age (Ma)	$^{207}\text{Pb}/^{235}\text{U}$ Age (Ma)	$^{207}\text{Pb}/^{206}\text{Pb}$ Age (Ma)
DVK-13-1	0.2753	318313	19000	0.0262	0.0002	0.1892	0.0024	0.0524	0.0005	166 ± 2	175 ± 2	295 ± 18
DVK-13-2	0.3698	431875	15000	0.0262	0.0002	0.2235	0.0080	0.0627	0.0021	166 ± 2	204 ± 7	641 ± 63
DVK-13-3	0.7870	906250	15530	0.0260	0.0002	0.2400	0.0042	0.0672	0.0013	165 ± 2	218 ± 4	822 ± 37
DVK-13-4	0.2640	300000	21700	0.0262	0.0002	0.2165	0.0043	0.0595	0.0006	166 ± 2	198 ± 4	578 ± 23
DVK-13-5	0.2740	316875	22700	0.0261	0.0002	0.2101	0.0019	0.0583	0.0004	166 ± 2	193 ± 2	541 ± 15
DVK-13-6	0.0740	99063	3000	0.0292	0.0010	0.7030	0.0790	0.1590	0.0120	185 ± 6	495 ± 43	2200 ± 140
DVK-13-7	0.3540	386250	16400	0.0250	0.0003	0.2189	0.0052	0.0638	0.0011	159 ± 2	201 ± 5	726 ± 36
DVK-13-8	0.5210	590625	23400	0.0259	0.0002	0.2309	0.0032	0.0644	0.0004	165 ± 2	210 ± 3	754 ± 14
DVK-13-9	0.3566	402125	25000	0.0257	0.0002	0.1935	0.0021	0.0545	0.0004	163 ± 1	179 ± 2	387 ± 17

Table 4

Hf isotope data for zircons in the metarhyodacite samples from the Çangaldağ Metamorphic Complex.

Grain#	$^{176}\text{Hf}/^{177}\text{Hf}$	SE	T _{DM} (Ma)	εHf	$^{176}\text{Lu}/^{177}\text{Hf}$	$^{173}\text{Yb}/^{177}\text{Hf}$	$^{178}\text{Hf}/^{177}\text{Hf}$	SE	Total Hf Int (V)
AK-7-2	0.28215	0.00002	1416	-22.5	0.00106	0.04997	1.46724	0.00003	3.67
AK-7-3	0.28267	0.00003	782	-4.0	0.00060	0.02676	1.46734	0.00005	2.86
AK-7-4	0.28276	0.00003	678	-1.0	0.00126	0.05913	1.46738	0.00004	3.56
AK-14-1	0.28277	0.00002	676	-0.6	0.00202	0.10426	1.46730	0.00004	4.05
AK-14-2	0.28280	0.00003	620	0.6	0.00135	0.05155	1.46725	0.00005	2.56
AK-14-3	0.28296	0.00003	413	6.2	0.00235	0.10601	1.46717	0.00006	2.77
AK-14-4	0.28281	0.00003	606	1.0	0.00149	0.06054	1.46729	0.00006	2.50
AK-14-5	0.28171	0.00004	2067	-38.1	0.00071	0.02710	1.46739	0.00005	2.71
AK-14-6	0.28204	0.00003	1623	-26.2	0.00071	0.03091	1.46736	0.00004	3.14
AK-22-1	0.28284	0.00003	566	2.0	0.00144	0.05791	1.46742	0.00005	1.99
AK-22-2	0.28272	0.00003	724	-2.1	0.00128	0.05549	1.46718	0.00005	3.02
AK-22-3	0.28281	0.00003	607	0.8	0.00109	0.04822	1.46747	0.00005	2.85
AK-22-4	0.28286	0.00004	538	2.7	0.00136	0.05842	1.46748	0.00006	2.19

Table 5

Hf isotope data for zircons in the Devrekani Metadiorite.

Grain#	$^{176}\text{Hf}/^{177}\text{Hf}$	SE	T _{DM} (Ma)	εHf	$^{176}\text{Lu}/^{177}\text{Hf}$	$^{173}\text{Yb}/^{177}\text{Hf}$	$^{178}\text{Hf}/^{177}\text{Hf}$	SE	Total Hf Int (V)
DV-11-1	0.28278	0.00003	671	-0.2	0.00257	0.09876	1.46723	0.00004	1.79
DV-11-3	0.28277	0.00003	660	-0.7	0.00084	0.03122	1.46732	0.00004	2.12
DV-11-4	0.28262	0.00002	864	-5.9	0.00111	0.04369	1.46726	0.00004	2.46
DV-11-5	0.28289	0.00003	517	3.8	0.00291	0.11981	1.46723	0.00004	2.01
DV-11-6	0.28263	0.00002	844	-5.5	0.00079	0.03274	1.46717	0.00004	3.12
DV-11-7	0.28281	0.00002	614	0.7	0.00141	0.05997	1.46725	0.00003	2.46
DV-11-8	0.28199	0.00002	1715	-28.1	0.00119	0.05208	1.46724	0.00003	3.06
DV-11-9	0.28262	0.00002	855	-5.7	0.00091	0.03548	1.46723	0.00003	2.64
DV-11-10	0.28279	0.00003	636	0.1	0.00126	0.04567	1.46730	0.00005	2.19
DV-11-11	0.28278	0.00002	658	-0.3	0.00167	0.06406	1.46725	0.00004	2.19

(Fig. 5); also shown in Fig. 5 is the position of the laser ablation spots and associated U-Pb ages. As shown on the Concordia ($^{206}\text{Pb}/^{238}\text{U}$ vs $^{207}\text{Pb}/^{235}\text{U}$) diagrams (Fig. 7), three similar Middle Jurassic ages of 176.4 ± 5.9 Ma for AK-7 (concordant age), 156.3 ± 2.9 Ma for AK-14 (lower intercept age), and 161 ± 12 Ma– 164 ± 13 Ma for AK-22

(weighted mean $^{206}\text{Pb}/^{238}\text{U}$ ages) were determined (Fig. 7). Recently, a U-Pb Middle Jurassic age of $(169 \pm 2$ Ma was also published for a single sample of metadacite from the CMC (Okay et al., 2014), and is consistent with the age determinations reported here. In addition to the Middle Jurassic ages, the presence of inherited/older zircons

Table 6

Hf isotope data for zircons in the granite sample from the Devrekani Granitoid.

Grain#	$^{176}\text{Hf}/^{177}\text{Hf}$	SE	T_{DM} (Ma)	ϵHf	$^{176}\text{Lu}/^{177}\text{Hf}$	$^{173}\text{Yb}/^{177}\text{Hf}$	$^{178}\text{Hf}/^{177}\text{Hf}$	SE	Total Hf Int (V)
DVK-13-1	0.28292	0.00003	463	4.9	0.00226	0.10018	1.46733	0.00005	2.17
DVK-13-3	0.28289	0.00002	493	3.8	0.00125	0.05383	1.46732	0.00004	2.13
DVK-13-4	0.28289	0.00003	551	3.9	0.00531	0.24329	1.46729	0.00004	1.85
DVK-13-5	0.28282	0.00004	590	1.2	0.00101	0.04511	1.46735	0.00006	1.34
DVK-13-6	0.28294	0.00005	434	5.6	0.00206	0.09090	1.46736	0.00007	1.45
DVK-13-7	0.28292	0.00005	456	4.9	0.00180	0.07666	1.46732	0.00007	1.03
DVK-13-8	0.28289	0.00006	513	3.8	0.00272	0.13028	1.46725	0.00007	1.49

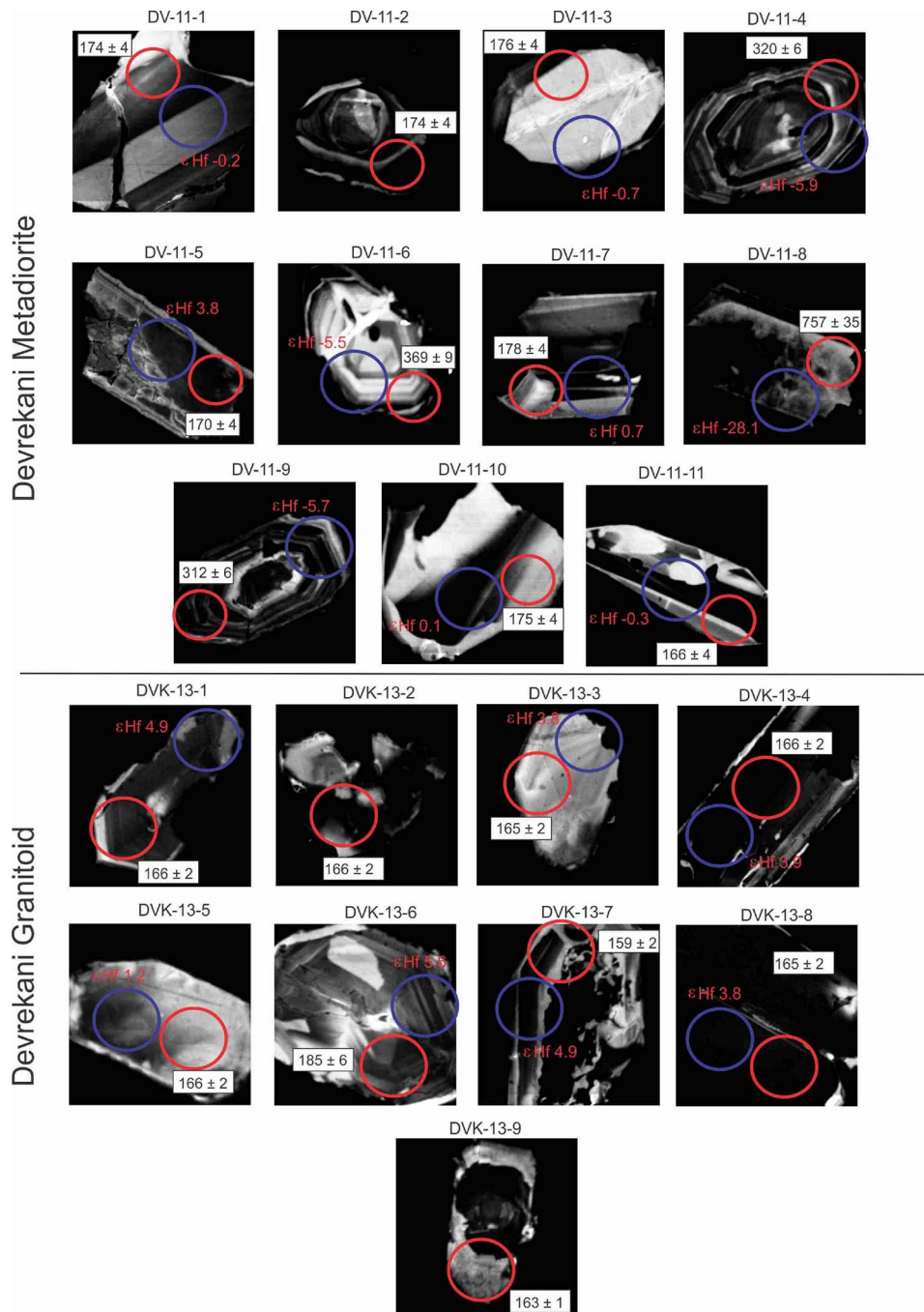


Fig. 6. CL images of zircon grains from metadiorite (sample DV-11) intruding the Devrekani Metaophiolite (Red circles: U-Pb ($^{207}\text{Pb}/^{235}\text{U}$ in Ma) spots-25 μm , Blue circles: Hf spots-35 μm) and from the Devrekani Granitoid (sample DVK-13)(Red circles: U-Pb ($^{207}\text{Pb}/^{235}\text{U}$ in Ma) spots-35 μm , Blue circles: Hf spots-35 μm) samples. (For interpretation of the references to colour in this figure legend, the reader is referred to the web version of this article.)

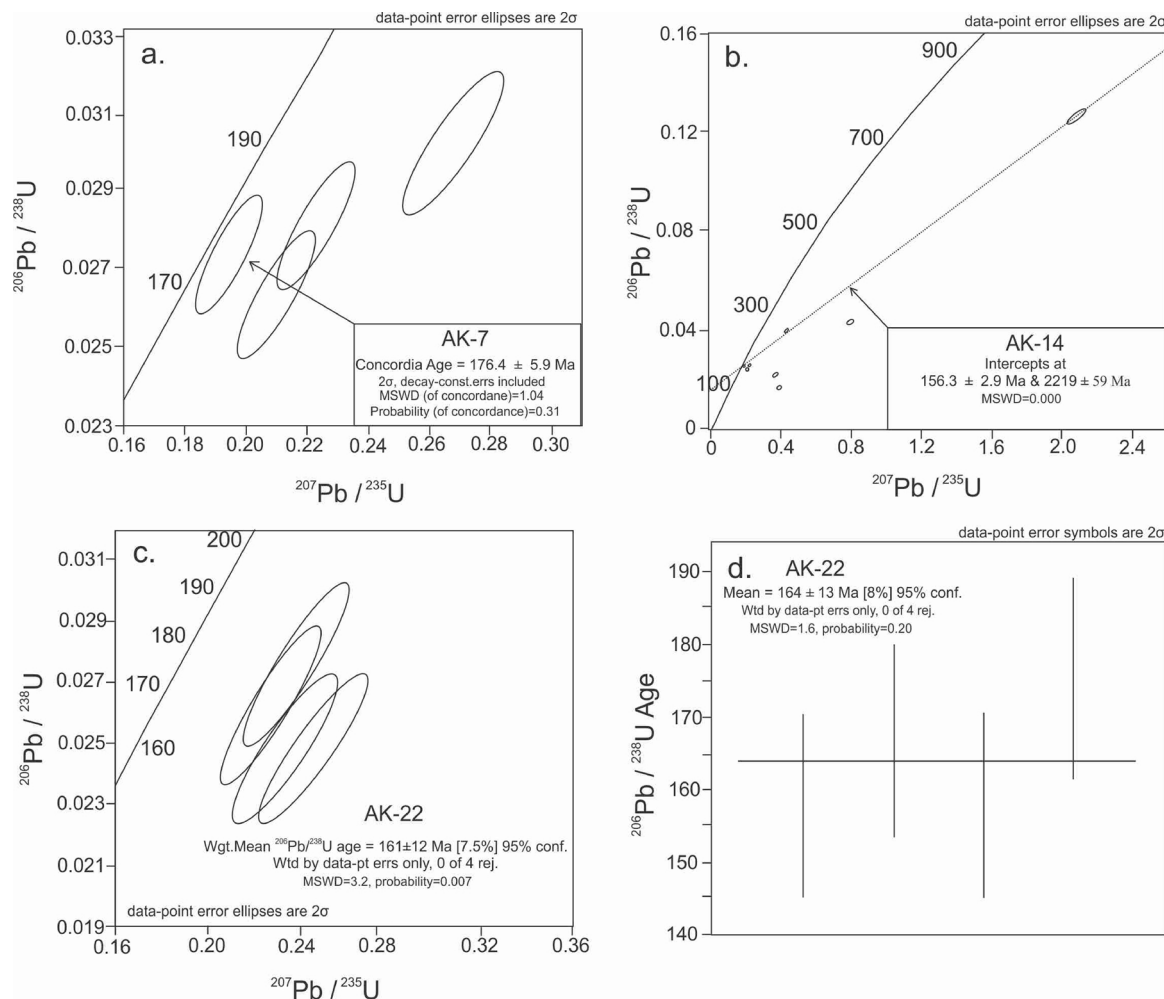


Fig. 7. $^{206}\text{Pb}/^{238}\text{U}$ vs $^{207}\text{Pb}/^{235}\text{U}$ diagrams for AK-7, AK-14 and AK-22 samples (Çangaldağ Metamorphic Complex). (A) Concordia age for AK-7 (B) Lower intercept age for AK-14 (C, D) Weighted mean age (analysis # 4) for AK-22.

(250 ± 3 Ma, 272 ± 2 Ma and 767 ± 14 Ma) implies that Triassic, Permian and Neoproterozoic rocks were present within the source of the protolith during arc magmatism.

4.1.2. Devrekani Metadiorite intruding the Devrekani Metaophiolite

On the basis of field relations, two metadiorite bodies intrude the Devrekani Metaophiolite (Fig. 4b). From these, metadiorite sample DV-11 yielded 11 zircon grains for analysis. The morphology of the analyzed zircons ranges from rounded to euhedral; structures may be diffused, oscillatory, laminated or unzoned; laser ablation spots and associated U-Pb ages are given in Fig. 6. The analytical data are reported in Table 2 and shown on the Concordia ($^{206}\text{Pb}/^{238}\text{U}$ vs $^{207}\text{Pb}/^{235}\text{U}$) diagram (Fig. 8a). A Middle Jurassic age of 163.3 ± 8.8 Ma (lower intercept age) was determined for the metadiorite. This age also provides a pre-Middle Jurassic relative age for the Devrekani Metaophiolite. The other important result is the evidence for post-Middle Jurassic-aged metamorphism since both units are metamorphosed. Also, the ages of inherited zircons vary from 312 ± 6 Ma to 757 ± 35 , which indicate the involvement of older crustal rocks (Late Carboniferous to Neoproterozoic).

4.1.3. Devrekani Granitoid

The Devrekani Granitoid is located to the south of the Devrekani town (Fig. 3). A total of 9 zircon grains were extracted from granite sample DVK-13. The morphology of the analysed zircons ranges from rounded to euhedral and internal structures may be diffuse, oscillatory, laminated or unzoned. The in-situ U-Pb age results and locations of

laser ablation spots are shown in Fig. 6. The data are given in Table 3 and shown on the Concordia diagram (Fig. 8b). A Middle Jurassic age of 164.9 ± 2.9 Ma (weighted mean $^{206}\text{Pb}/^{238}\text{U}$ age) was determined for this granite as well (Fig. 8c).

4.2. Hf isotope systematics

4.2.1. Çangaldağ Metamorphic Complex

The Lu-Hf geochronometer is one of the useful isotope systems in order to evaluate mantle source(s) and determine depleted mantle (T_{DM}) model age(s) (e.g., Schmidberger et al., 2005; Simonetti and Neal, 2010). Zircon grains from three meta-rhyodacite samples (AK-7, AK-14, and AK-22) within the CMC were analyzed and the results are shown on initial $^{176}\text{Hf}/^{177}\text{Hf}$ (and ϵHf) vs time diagrams (Fig. 9). The initial $^{176}\text{Hf}/^{177}\text{Hf}$ ratios, T_{DM} model ages, ϵHf values and corresponding laser ablation spots are given in Table 4. In-situ $^{176}\text{Hf}/^{177}\text{Hf}$ initial ratios range between 0.28171 ± 0.00004 and 0.28296 ± 0.00003 , and correspond to T_{DM} model ages between 2067 and 413 Ma. Of interest, the effect of low-grade metamorphism (greenschist facies) and hydrothermal alteration may cause Pb-loss within zircon, and leads to shifting points to the left (horizontally) within Fig. 9, which may result in misinterpretation of the data; i.e., imply derivation from a more radiogenic (enriched) source region. The calculated ϵHf values are between -38.1 and 6.2 for the metarhyodacite samples (AK-7, AK-14 and AK-22), which may be attributed to the mixing of magmas derived from both depleted mantle and oceanic crustal sources (Vervoort et al., 1999; Kröner et al., 2014; Çimen et al.,

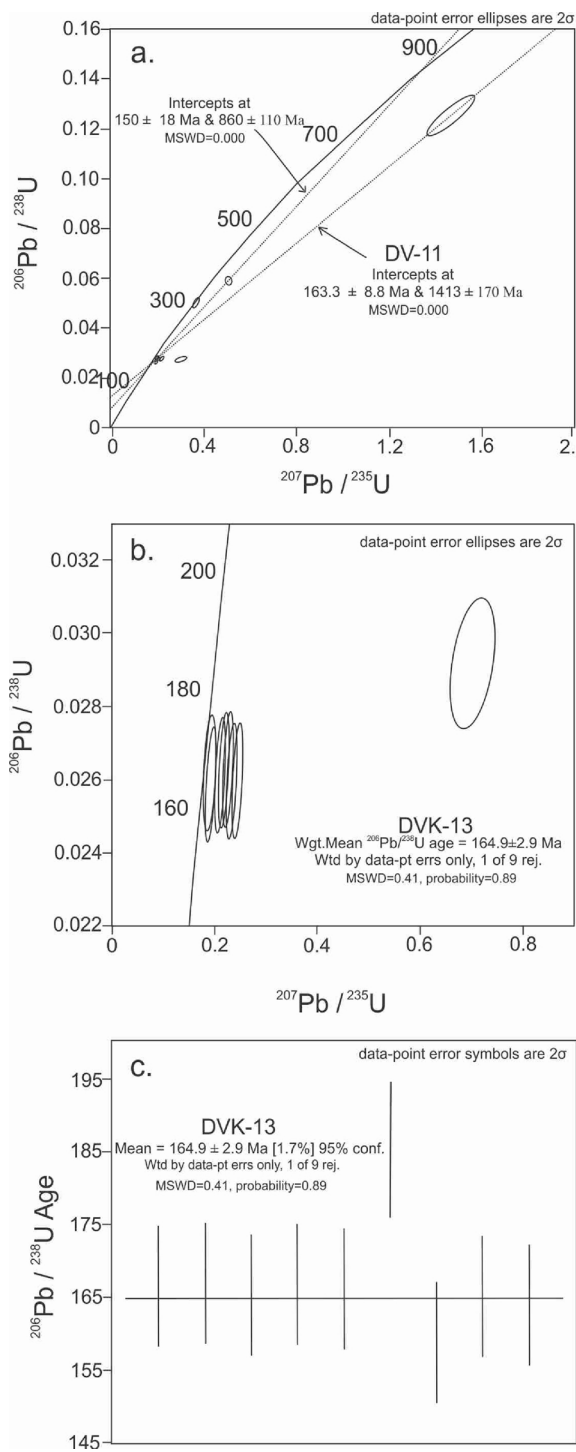


Fig. 8. $^{206}\text{Pb} / ^{238}\text{U}$ vs $^{207}\text{Pb} / ^{235}\text{U}$ diagrams for DV-11 (Metadiorite intruding Devrekani Metaophiolite) and DVK-13 (Devrekani Granitoid) samples. (A) Lower intercept age for DV-11 (B, C) Weighted mean age (analysis # 9) for DVK-13.

2017).

4.2.2. Devrekani Metadiorite and Granitoid

The Hf isotope results for zircon grains from the metadiorite (DV-11) and granite (DVK-13) are shown in Fig. 10. The $^{176}\text{Hf} / ^{177}\text{Hf}$ initial ratios, T_{DM} model ages, ϵHf values and laser ablation spots are given in Tables 5 and 6. The average in-situ $^{176}\text{Hf} / ^{177}\text{Hf}$ initial ratio is 0.28267 ± 0.00002 for the metadiorite sample, which corresponds to a 803 Ma T_{DM} model age. The average ϵHf value is ~ -4 for this sample. In addition, the average $^{176}\text{Hf} / ^{177}\text{Hf}$ initial ratio for the granite

is 0.28289 ± 0.00004 , and corresponds to a 500 Ma T_{DM} model age; the calculated average ϵHf value is also $\sim +4$ for the granite sample, and this value indicates derivation from a more depleted mantle source compared to the metadiorite sample. The calculated T_{DM} model ages for these units indicate that Middle Jurassic magmatism resulted from partial melting of Cambrian and Neoproterozoic rocks. Similar ages were reported from cores of zircons derived from the Çangaldağ pluton intruding the pre-Middle Jurassic structural units of the Eurasian margin (Çimen et al., 2017).

4.3. Geological and geodynamic constraints

The new petrological data including U-Pb geochronology and Lu-Hf systematics reported in this paper in relation to the CMC, Devrekani Metadiorite and Granitoid play an important role towards understanding the geodynamic evolution of the CP and Black Sea region. The CP (Fig. 2a) consists of pre-Jurassic basement units (e.g. Devrekani Metamorphics, Gemi Complex and Permo-Carboniferous Deliktaş-Sivrikaya Granitoids), the Early Jurassic accretionary prism (Küre Complex), and the widespread Middle Jurassic continental magmatism (e.g., Devrekani Granitoid, Çangaldağ and Karaman Plutons).

The CP includes several oceanic units such as the CMC, Domuzdağ, Aylı Dağ, Arkot Dağ, Emirköy, Saka and Daday (e.g. Ustaömer and Robertson, 1999; Okay et al., 2006, 2013, Göncüoğlu et al., 2012, 2014; Tekin et al., 2012; Marroni et al., 2014; Sayit et al., 2016; Frassi et al., 2016). Late Jurassic-Early Cretaceous metamorphic ages have been assigned for some tectonic units (e.g. Domuzdağ Unit, Saka Unit, Daday Unit, Okay et al., 2006, 2013; Marroni et al., 2014). Additionally, Middle Bathonian to Callovian ages have been determined for radiolarian cherts within the Aylı Dağ Unit (Göncüoğlu et al., 2012). Overall, geochemical and tectono-metamorphic characteristics of the oceanic assemblages (e.g. CMC, Domuz Dağ, Aylı Dağ and Daday Units) indicate that they could have formed in a supra-subduction zone (Okay et al., 2006, 2013; Günay et al., 2016; Sayit et al., 2016; Frassi et al., 2016; Çimen et al., 2016). The age and isotope data from the CMC also support the interpretation that magmatism may have formed in an intra-oceanic subduction zone generated by mixing of mantle and oceanic crustal rocks during the Middle Jurassic.

In addition to the oceanic units, the Middle Jurassic continental magmatism (e.g. Devrekani Granitoid, Çangaldağ and Karaman Plutons) intrudes the basement units (e.g. Devrekani and Gemi Complexes) and the Early Jurassic accretionary prism (Küre Complex) in the CP (Fig. 2a). Hence, the Çangaldağ Pluton represents an active arc located above the subducting slab of the IPO beneath the accreted basement of the CP. It must be noted that the petrological data from the Çangaldağ Pluton imply that this arc magmatism may have involved partial melting of Neoproterozoic/Mesoproterozoic crustal rocks (Çimen et al., 2017), a common feature of Gondwana-derived terranes. Similar to this unit, the age and isotope data reported here indicate that the Devrekani Metadiorite and Devrekani Granitoid could have source components formed by partial melting of Cambrian and Neoproterozoic basement rocks of the Eurasian margin during the Middle Jurassic.

Jurassic magmatic rocks also outcrop in the western part of the SCT and Eastern Pontides in Turkey (Fig. 1; Çimen et al., 2017). The Early to Middle Jurassic Mudurnu volcanics in the western SCT display sub-alkaline and calc-alkaline geochemical affinities and are akin to the rift-related magmatism (Genc and Tuysuz, 2010). Moreover, the Early Jurassic Demirkent Complex intrudes the Carboniferous metamorphic basement rocks of the SCT in the Eastern Pontides (e.g. Artvin-Yusufeli area), and these exhibit calc-alkaline and tholeiitic affinity, similar to those found within a continental rift environment (Dokuz et al., 2010 and the references therein). According to a recent study (Dokuz et al., 2017 and the references therein); the Late Jurassic magmatism in the Eastern Sakarya Zone is possibly the result of slab breakoff of Paleotethyan oceanic lithosphere.

Jurassic arc-type volcanic rocks have been defined in the Crimea

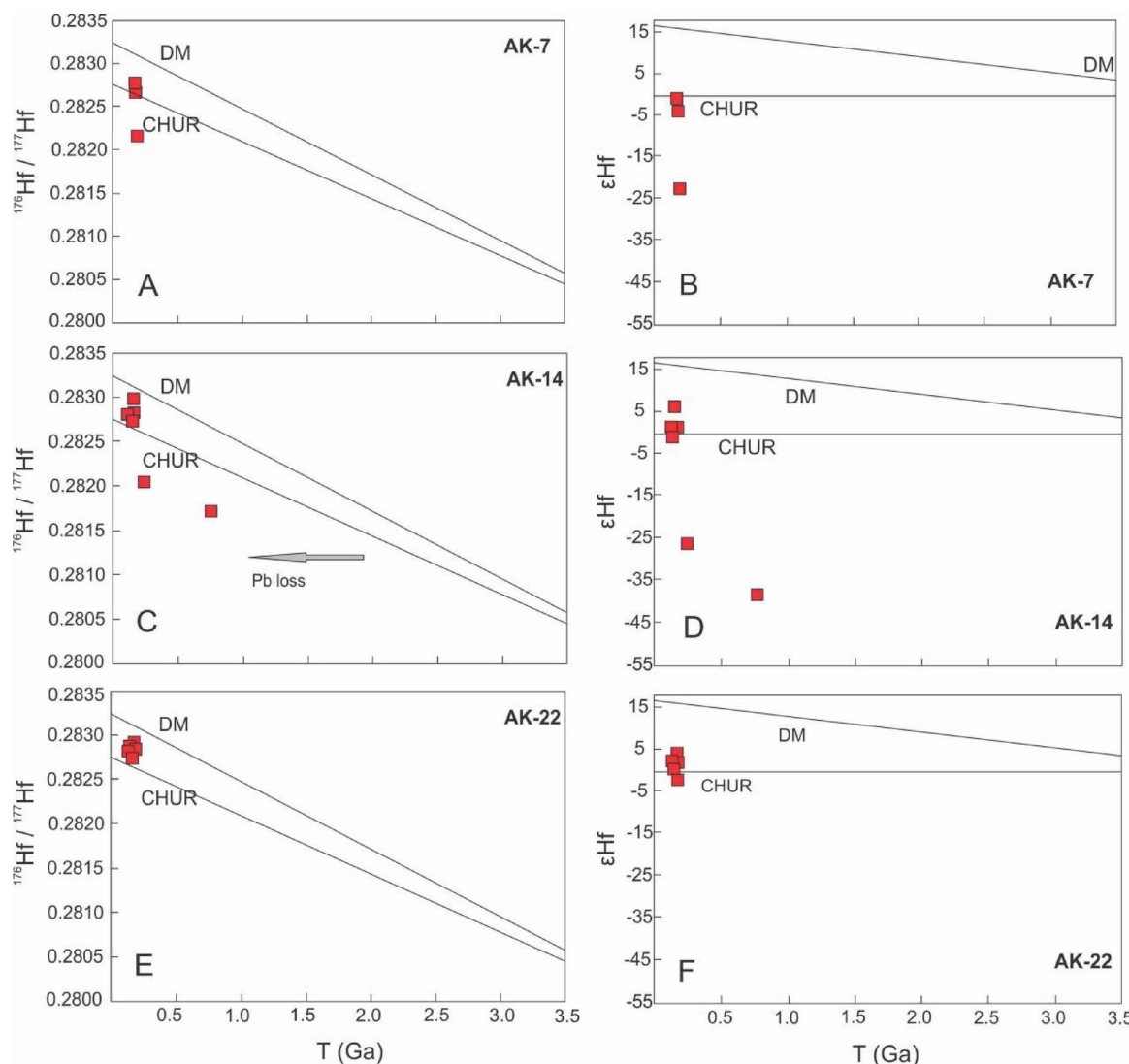


Fig. 9. $^{176}\text{Hf}/^{177}\text{Hf}$ (A, C, E) and ϵHf (B, D, F) vs Time diagrams for AK-7, AK-14 and AK-22 samples (Çangaldağ Metamorphic Complex). The ϵHf and TDM age values were calculated using the following formulas; $\epsilon\text{Hf} = [(^{176}\text{Hf}/^{177}\text{Hf})_{\text{SMP}} / (^{176}\text{Hf}/^{177}\text{Hf})_{\text{CHUR}} - 1] \times 10^4$; $\text{Hf T}_{\text{DM}} = 1/\lambda \times \ln x \times [(^{176}\text{Hf}/^{177}\text{Hf})_{\text{SMP}} - (^{176}\text{Hf}/^{176}\text{Hf})_{\text{DM}} / (^{176}\text{Lu}/^{177}\text{Hf})_{\text{SMP}} - (^{176}\text{Lu}/^{176}\text{Hf})_{\text{DM}} + 1]$. Here, $^{176}\text{Lu}/^{177}\text{Hf}_{\text{DM}} = 0.0384$ (Griffin et al., 2002). $^{176}\text{Hf}/^{177}\text{Hf}_{\text{DM}} = 0.28325$ (Griffin et al., 2002). $^{176}\text{Hf}/^{177}\text{Hf}_{\text{CHUR}} = 0.282785$ (Bouvier et al., 2008). For age correction: $^{176}\text{Hf}/^{177}\text{Hf}_{\text{in}} = ^{176}\text{Hf}/^{177}\text{Hf}_{\text{meas}} - ^{176}\text{Lu}/^{177}\text{Hf} (\text{e}^{\lambda t} - 1)$. $\lambda = 1.867 \times 10^{-11} \text{ yr}^{-1}$ (Scherer et al., 2001).

region (Fig. 2b; in the Bodrak/Simferopol areas). These volcanic rocks could have formed in a subduction-related setting under an accreted active margin of Eurasia (Meijers et al., 2010). Similar Jurassic volcanic rocks (e.g. the Kirar diorite intruded into the Dizi Series; Somin, 2011), which display geochemical characteristics of subduction-related rock types have been reported in the Greater Caucasus (Fig. 2c; McCann et al., 2010). All of these evidences from the CP, Crimea, the Great Caucasus, the western SCT, Eastern Pontides and Lesser Caucasus suggest that there was an active subduction system in these regions during the Jurassic period.

Based upon all regional geological and petrological evidences and our new age and Hf isotope data, the CP includes the remnants of the IPO that was closed by multiple subduction systems (e.g. Çimen et al., 2017) during the Middle Jurassic (Fig. 11). In this preferred model, the Variscan Basement comprises the Devrekani Metamorphics, Geme Complex and Permo-Carboniferous Deliktaş-Sivrikaya Granitoids. The southerly located subduction in this model may result in formation of the supra-subduction type arc magmatics of the CMC generated on the arc-back-arc volcanics (Aylı Dağ ophiolite, Arkot Dağ melange and the Domuzdağ, Saka and Daday units of Göncüoğlu et al., 2012; Sayit et al., 2016). The northern subduction system may have caused generation of

the continental margin magmatism (e.g. Devrekani Granitoid, Çangaldağ and Karaman Plutons; Fig. 11). As evidenced by Ar–Ar white mica ages (Okay et al., 2013), the accretion and metamorphism of the volcanic assemblages from the fore-arc, the island arc and the back-arc occurred during the Early Cretaceous (Valanginian-Barremian). The final closure of the IPO occurred during the Late Paleocene-Early Eocene time and its remnants have been tectonically emplaced to the south onto the SCT (e.g. Göncüoğlu et al., 2000; Catanzariti et al., 2013, Ellero et al., 2015; Çimen et al., 2016).

5. Conclusions

The northern CP comprises pre-Jurassic basement units (e.g. Devrekani Metamorphics, Geme Complex and Permo-Carboniferous Deliktaş-Sivrikaya Granitoids), the Early Jurassic accretionary prism (Küre Complex), and the widespread Middle Jurassic continental magmatism (e.g. Devrekani Granitoid, Çangaldağ and Karaman Plutons). The basement units are cut by the widespread Middle Jurassic magmatism at several locations, which represents a continental arc, formed by the northward subduction of the IPO beneath the Eurasian margin. In addition to the CP, the presence of similar Jurassic magmatic

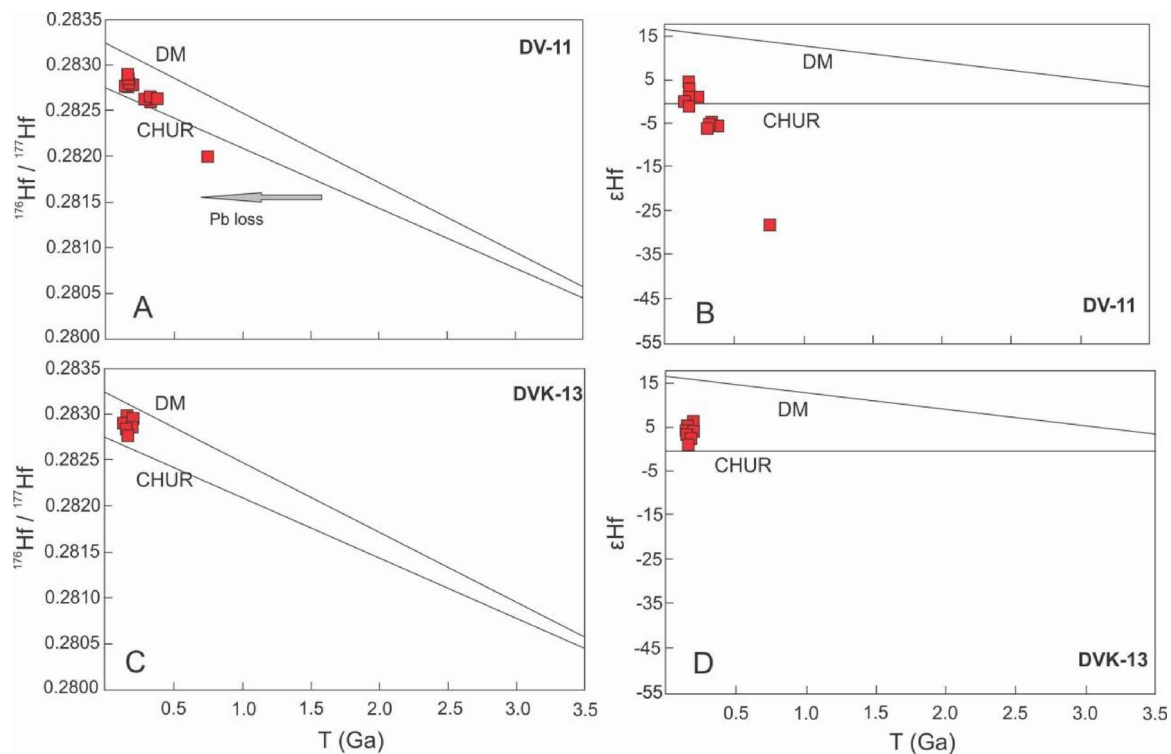


Fig. 10. $^{176}\text{Hf} / ^{177}\text{Hf}$ (A, C) and ϵHf (B, D) vs Time diagrams for DV-11 (Devrekani Metadiorite) and DVK-13 (Devrekani Granitoid) samples. Calculations are same as shown in Fig. 10.

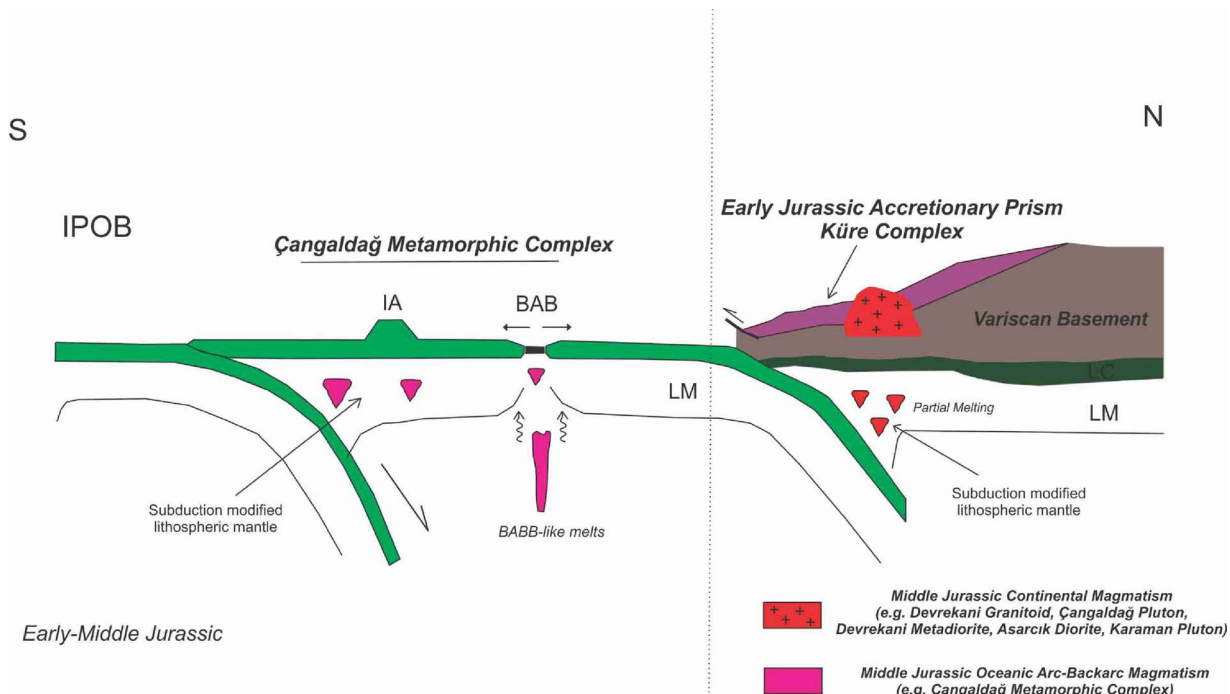


Fig. 11. Proposed geodynamic model for the Middle Jurassic oceanic and continental magmatism in the Central Pontides (modified from Çimen (2016) and Çimen et al. (2017); Variscan Basement: Devrekani Units, Gemi Complex, Sivrikaya and Deliktaş Granitoids; LM: Lithospheric Mantle; IA: Island Arcs; BAB: Back-arc Basin Basalt; LC: Lower Crust).

rocks is also known in the western part of SCT, Eastern Pontides, Crimea, Caucasus, and Iran. In contrast, the southern CP consists of the CPSC, a large Early Cretaceous subduction-accretion complex (e.g. CMC, Domuz Dağ Unit, Ayli Dağ Unit and Daday Unit), representing the remnants of the IPO. From these, the CMC is characterized by imbricated metavolcanic and metasedimentary rocks of arc-basin origin. Overall, radiometric age and isotope data from the oceanic (CMC) and

continental arc (Devrekani Metadiorite and Granitoid) units in the CP suggest the presence of a multiple subduction system within the Intrapontide branch of Neotethyan Ocean during the Middle Jurassic. In addition, the presence of similar Jurassic magmatic rocks in the regions of Crimea, Great Caucasus, western SCT, Eastern Pontides, and Lesser Caucasus are consistent with the occurrence of a subduction regime.

Acknowledgements

This research was supported by Higher Educational Council of Turkey, OYP-PhD grant, The Scientific and Technological Research Council of Turkey, 114Y422 project, and University of Notre Dame. The authors also gratefully acknowledge Çağrı Alperen İnan, Alican Aktaş and Uğur Balçı for their field assistance, and Drs. Ian Steele, Elizabeth C. Koeman, and Zehra Deveci for their laboratory assistance. Also, Dr. Irina Artemieva and two anonymous reviewers are sincerely acknowledged for their valuable suggestions and comments, which has resulted in an improved manuscript.

Appendix A. Supplementary data

Supplementary data associated with this article can be found, in the online version, at <https://doi.org/10.1016/j.jog.2018.01.004>.

References

- Çimen, O., Göncüoğlu, M.C., Sayit, K., 2016. Geochemistry of the meta-volcanic rocks from the Çangaldağı Complex in Central Pontides: implications for the Middle Jurassic arc – back – arc system in the Neotethyan Intra-Pontide Ocean. *Turkish J Earth Sci.* 25, 491–512.
- Çimen, O., Göncüoğlu, M.C., Simonetti, A., Sayit, K., 2017. Whole rock geochemistry, zircon U-Pb and Hf isotope systematics of the Çangaldağı pluton: evidences for middle jurassic continental arc magmatism in the Central Pontides, Turkey. *Lithos* 288–289C, 35–54.
- Çimen, 2016. The Petrology And Geochronology of the Igneous Rocks from the Çangaldağı Metamorphic Complex and the Çangaldağı Pluton (Central Pontides-Turkey), Central Pontides. Middle East Technical University (PhD Thesis, 254 p.).
- Şengör, A.M.C., Yilmaz, Y., 1981. Tethyan evolution of Turkey: a plate tectonic approach. *Tectonophysics* 75, 181–241.
- Sengün, M., Akçaoğlu, F., Keskin, H., Akat, U., Altun İ., E., Deveciler, E., Sevin, M., Armağan, F., Erdoğan, K., Acar Ş., Gündüz, H., 1988. Daday-Kastamonu-Inebolu yörensinin Jeolojisi, MTA Raporu, No: 8994. (unpublished, in Turkish).
- Aygül, M., Okay, A.I., Oberhänsli, R., Sudo, M., 2016. Pre-collisional accretionary growth of the southern Laurasian active margin Central Pontides, Turkey. *Tectonophysics* 671, 218–234.
- Bonhomme, M.G., Yilmaz, O., 1984. First K-Ar data from the Daday-Devrekani and İlgaz massifs and the Kastamonu granitoid belt, northern Turkey. *Terra Cognita* 4 (2), 199–200.
- Bouvier, A., Vervoort, J.D., Patchett, P.J., 2008. The Lu-Hf and Sm-Nd isotopic composition of CHUR: Constraints from unequilibrated chondrites and implications for the bulk composition of terrestrial planets. *Earth Planet. Sci. Lett.* 273, 48–57.
- Boztuğ, D., Yılmaz, O., 1995. Daday-Devrekani masif metamorfizması ve jeolojik evrimi, Kastamonu bölgesi, Batı Pontilder, Türkiye. *TJK Bülteni* 38, 33–52 (in Turkish).
- Boztuğ, D., Debon, F., Le Fort, P., Yılmaz, O., 1995. High compositional diversity of the middle Jurassic Kastamonu plutonic belt: Northern Anatolia, Turkey. *Turk. J. Earth Sci.* 4, 67–86.
- Catanzariti, R., Ellero, A., Göncüoğlu, M.C., Marroni, M., Ottria, G., Pandolfi, L., 2013. The Taraklı Flysch in the Boyalı area (Sakarya Terrane, northern Turkey): implications for the tectonic history of the intra-pontide suture zone. *C. R. Geosci.* 345, 454–461.
- Dokuz, A., Karsli, O., Chen, B., Uysal, İ., 2010. Sources and petrogenesis of Jurassic granitoids in the Yusufeli area, Northeastern Turkey: implications for pre-and post-collisional lithospheric thinning of the eastern Pontides. *Tectonophysics* 480, 259–279.
- Dokuz, A., Aydinçakır, E., Kandemir, R., Karslı, O., Siebel, W., Derman, A.M., Turan, M., 2017. Late Jurassic magmatism and stratigraphy in the Eastern Sakarya zone, Turkey: evidence for the slab Breakoff of paleotethyan oceanic lithosphere. *J. Geol.* 125, 1–31.
- Ellero, A., Ottria, G., Sayit, K., Catanzariti, R., Frassi, C., Göncüoğlu, M.C., Marroni, M., Pandolfi, L., 2015. Geological and geochemical evidence for a Late Cretaceous continental arc in the central Pontides, northern Turkey. *Ophioliti* 40, 73–90.
- Frassi, C., Göncüoğlu, M.C., Marroni, M., Pandolfi, L., Ruffini, L., Ellero, A., Ottria, G., Sayit, K., 2016. The intra-pontide suture zone in the Tosya-Kastamonu area, Northern Turkey. *J. Maps* 1, 211–219.
- Frassi, C., Marroni, M., Pandolfi, L., Göncüoğlu, M.C., Ellero, A., Ottria, G., Sayit, K., McDonald, C.S., Balestrieri, M.L., Malasoma, A., 2018. Burial and exhumation history of the Daday Unit (Central Pontides, Turkey): implications for the closure of the Intra-Pontide oceanic basin. *Geol. Mag.* 155, 356–376. <http://dx.doi.org/10.1017/S0016756817000176>.
- Göncüoğlu, M.C., Kozlu, H., Dirik, K., 1997. Pre-alpine and alpine terranes in Turkey: explanatory notes to the terrane map of Turkey. *Ann. Geol. Pays Hell.* 37, 515–536.
- Göncüoğlu, M.C., Turhan, N., Sentürk, K., Özcan, A., Uysal, S., 2000. A geotraverse across NW Turkey: tectonic units of the Central Sakarya region and their tectonic evolution. In: In: Bozkurt, E., Winchester, J.A., Piper, J.D. (Eds.), *Tectonics and Magmatism in Turkey and the Surrounding Area* 173. *Geol. Soc. London Spec. Publ.*, pp. 139–162.
- Göncüoğlu, M.C., Marroni, M., Sayit, K., Tekin, U.K., Ottria, G., Pandolfi, L., Ellero, A., 2012. The Aylı Dağ ophiolite sequence (Central-Northern Turkey): A fragment of Middle Jurassic Oceanic Lithosphere within the Intra-Pontide suture zone. *Ophioliti* 37, 77–92.
- Göncüoğlu, M.C., Marroni, M., Pandolfi, L., Ellero, A., Ottria, G., Catanzariti, R., Tekin, U.K., Sayit, K., 2014. The Arkot Dağ Melange in Araç area, central Turkey: evidence of its origin within the geodynamic evolution of the intra-pontide suture zone. *J. Asian Earth Sci.* 85, 117–139.
- Göncüoğlu, M.C., 2010. Introduction to the Geology of Turkey: Geodynamic Evolution of the Pre-Alpine and Alpine Terranes. MTA, pp. 1–69.
- Güler, M.A., Arslan, M., Sherlock, S., Heaman, L.M., 2016. Permo-carboniferous granitoids with jurassic high temperature metamorphism in Central Pontides, Northern Turkey. *Mineral. Petrol.* 110, 943–964.
- Günay, K., Dönmez, C., Uysal, İ., Yıldırım, N., Şahin, M.B., Yıldırım, E., Tablaci, A., Kang, J., Lee, I., 2016. Chrome spinel geochemistry of ultramafic rocks from the Elekdağ metaophiolite (Northern Turkey): implications for greenschist to mid-amphibolite facies metamorphism. *Neu Jb Mineral Abh.* 193, 1–16.
- Genc, S.C., Tuysuz, O., 2010. Tectonic setting of the Jurassic bimodal magmatism in the Sakarya Zone (Central and Western Pontides), Northern Turkey: a geochemical and isotopic approach. *Lithos* 118, 95–111.
- Griffin, W.L., Wang, X., Jackson, S.E., Pearson, N.J., O'Reilly, S.Y., Xu, X., Zhou, X., 2002. Zircon chemistry and magma mixing, SE China: in situ analysis of Hf isotopes, Tonglu and Pingtan igneous complexes. *Lithos* 61, 237–269.
- Jackson, S.E., Pearson, N.J., Griffin, W.L., Belousova, E.A., 2004. The application of laser ablation-inductively coupled plasma-mass spectrometry to in situ U-Pb zircon geochronology. *Chem. Geol.* 211, 47–69.
- Konya, S., Pehlivanoğlu, H., Tesrekli, M., 1988. Kastamonu, Taşköprü, Devrekani yöresi jeokimya raporu MTA (in Turkish). Report Number: 8341.
- Kozur, H., Aydin, M., Demir, O., Yakar, H., Göncüoğlu, M.C., Kuru, F., 2000. New stratigraphic results from the Paleozoic and Early Mesozoic of the Middle Pontides (Northern Turkey). *Geol. Croat.* 53, 209–268.
- Kröner, A., Hoffmann, J.E., Xie, H., Münker, C., Hegner, E., Wan, Y., Hofmann, A., Liu, D., Yang, J., 2014. Generation of early Archaean grey gneisses through melting of older crust in the eastern Kaapvaal craton, southern Africa. *Precambrian Res.* 255, 823–846.
- Marroni, M., Frassi, C., Göncüoğlu, M.C., Di Vincenzo, G., Pandolfi, L., Rebay, G., Ellero, A., Ottaria, G., 2014. Late Jurassic amphibolite-facies metamorphism in the Intra-Pontide SutureZone (Turkey): an eastward extension of the Vardar Ocean from the Balkans into Anatolia? *J. Geol. Soc.* 171, 605–608.
- McCann, T., Chalot-Prat, F., Saintot, A., 2010. The Early Mesozoic evolution of the Western Greater Caucasus (Russia): Triassic-Jurassic sedimentary and magmatic history. *Geol. Soc. London Spec. Publ.* 340, 181–238.
- Meijers, M.J.M., Vrouwe, B., van Hinsbergen, D.J.J., 2010. Jurassic arc volcanism on Crimea (Ukraine): implications for the paleo-subduction zone configuration of the Black Sea region. *Lithos* 119, 412–426.
- Nzegge, O., 2008. Petrogenesis and Geochronology of the Deliktaş, Sivrikaya and Devrekani Granitoids and Basement, Kastamonu Belt-central Pontides (nw Turkey): Evidence for Late Paleozoic-mesozoic Plutonism, and Geodynamic Interpretation. PhD Thesis. (p. 177).
- Okay, A.I., Nikishin, M.A., 2015. Tectonic evolution of the southern margin of Laurasia in the Black Sea region. *Int. Geol. Rev.* 57, 1051–1076.
- Okay, A.I., Tuysuz, O., 1999. In: Durand, B., Jolivet, L., Horvath, F., Seranne, M. (Eds.), *Tethyan Sutures of Northern Turkey*. In: *The Mediterranean Basins: Tertiary Extension Within the Alpine Orogen* 156. *Geol. Soc. London Spec. Publ.*, pp. 475–515.
- Okay, A.I., Tuysuz, O., Satur, M., Özkan-Altiner, S., Altiner, D., Sherlock, S., Eren, R.H., 2006. Cretaceous and Triassic subduction-accretion, high-pressure-low-temperature metamorphism, and continental growth in the Central Pontides, Turkey. *Geol. Soc. Am. Bull.* 118, 1247–1269.
- Okay, A.I., Gürsel, S., Sherlock, S., Altiner, D., Tuysuz, O., Kylander-Clark, A.R.C., Aygül, M., 2013. Early Cretaceous sedimentation and orogeny on the active margin of Eurasia: Southern Central Pontides, Turkey. *Tectonics* 32, 1247–1271.
- Okay, A.I., Gürsel, S., Tuysuz, O., Sherlock, S., Keskin, M., Kylander-Clark, A.R.C., 2014. Low-pressure – high-temperature metamorphism during extension in a Jurassic magmatic arc Central Pontides, Turkey. *J. Metamorph. Geol.* 32, 49–69.
- Okay, A.I., Altiner, D., Kılıç, A., 2015. Triassic limestone, turbidites and serpentinite—the Cimmerian orogeny in the Central Pontides. *Geol. Mag.* 152, 460–479.
- Robertson, A.H.F., Ustaömer, T., 2004. Tectonic evolution of the Intra-Pontide suture zone in the Artmutlu Peninsula, NW Turkey. *Tectonophysics* 381, 175–209.
- Robertson, A., Parlak, O., Ustaömer, T., Tash, K., İnan, N., Dumitrica, P., Karaoglu, F., 2013. Subduction, ophiolite genesis and collision history of Tethys adjacent to the Eurasian continental margin: new evidence from the Eastern Pontides, Turkey. *Geodin. Acta* 26 (3–4), 1–64.
- Sarifakioğlu, E., Dilek, Y., Sevin, M., Pehlivanoğlu, K., Kandemir, Ö., Möller, A., Bayanova, T., Uysal, İ., Keles, M., 2017. Permo-Triassic and Liassic Tethyan oceanic tracts within the Pontide Belt along the southern margin of Eurasia, Northern Anatolia. *Acta Geol. Sin. (English Edition)* 91, 33–34.
- Sayit, K., Marroni, M., Göncüoğlu, M.C., Pandolfi, L., Ellero, A., Ottria, G., Frassi, C., 2016. Geological setting and geochemical signatures of the mafic rocks from the intra-Pontide Suture Zone: implications for the geodynamic reconstruction of the Mesozoic Neotethys. *Int. J. Earth Sci.* 105, 39–64.
- Scherer, E.E., Münker, C., Mezger, K., 2001. Calibration of the Lu-Hf clock. *Science* 293, 683–687.
- Schmidberger, S.S., Heaman, L.M., Simonetti, A., Creaser, R.A., Cookenboo, H.O., 2005. Formation of Paleoproterozoic eclogitic mantle, Slave province (Canada): insights from in-situ Hf and U-Pb isotope analyses of mantle zircons. *Earth Planet. Sci. Lett.* 240, 621–633.
- Simonetti, A., Neal, C.R., 2010. In-situ chemical U-Pb dating and Hf isotope investigation

- of megacrystic zircons, Malaita (Solomon Islands): evidence for multiple stage alkali magmatic activity beneath the Ontong Java Plateau. *Earth Planet. Sci. Lett.* 295, 251–261.
- Simonetti, A., Heaman, L.R., Hartlaub, R., Creaser, T., MacHattie, T.G., Böhm, C., 2005. U-Pb zircon dating by laser ablation-MC-ICP-MS using a new multiple ion counting Faraday collector array. *J. Anal. At. Spectrom.* 20, 677–686.
- Slama, J., Kosler, J., Condon, D.J., Crowley, J.L., Gerdes, A., Hanchar, J.M., Horstwood, M.S.A., Morris, G.A., Nasdala, L., Norberg, N., Schaltegger, U., Schoene, N., Tubrett, M.N., Whitehouse, M.J., 2008. Plesovice zircon – a new natural reference material for U-Pb and Hf isotopic microanalysis. *Chem. Geol.* 249 (1–2), 1–35.
- Solov'ev, A.V., Rogov, M.A., 2010. First FissionTrack dating of zircons from mesozoic complexes of the crimea. *Stratigr. Geol. Correl.* 18, 298–306.
- Stampfli, G.M., Borel, G.D., 2002. A plate tectonic model for the Palaeozoic and Mesozoic constrained by dynamic plate boundaries and restored synthetic oceanic isochrones. *Earth Planet. Sci. Lett.* 169, 17–33.
- Somin, M.L., 2011. Pre-Jurassic basement of the greater caucasus: brief overview. *Turkish J. Earth Sci.* 20, 545–610.
- Tüysüz, O., 1985. Kargı Masifi ve dolayındaki tektonik birliklerin ayrıldı ve araştırılması (petrolojik inceleme). Doktora tezi, İstanbul Üniversitesi, Fen Bilimleri Enstitüsü, 431 s. (in Turkish).
- Tüysüz, O., 1990. Tectonic evolution of a part of the Tethyside orogenic collage: the Kargı Massif, northern Turkey. *Tectonics* 9, 141–160.
- Tekin, U.K., Göncüoğlu, M.C., Pandolfi, L., Marroni, M., 2012. Middle Late Triassic radiolarian cherts from the Arkotdağ melange in northern Turkey: implications for the life span of the northern Neotethyan branch. *Geodin. Acta* 25, 305–319.
- Uğuz, M.F., Sevin, M., 2007. Türkiye Jeoloji Haritaları, Kastamonu-E32 Paftası. *Jeoloji Etütleri Dairesi*, 32 s. (in Turkish).
- Ustaömer, T., Robertson, A.H.F., 1999. Geochemical evidence used to test alternative plate tectonic models for pre-Upper Jurassic (Palaeotethyan) units in the Central Pontides, N Turkey. *Geol. J.* 34, 25–53.
- Vervoort, J.D., Patchett, P.J., Blachert-Toft, J., Albarede, F., 1999. Relationship between Lu-Hf and Sm-Nd systems in the global sedimentary system. *Earth Planet. Sci. Lett.* 168, 79–99.
- Wiedenbeck, M., Alle, P., Corfu, F., Griffin, W.L., Meier, M., Oberli, F., von Quadt, A., Roddick, J.C., Spiegel, W., 1995. Three natural zircon standards for U-Th-Pb, Lu-Hf, trace element and REE analyses. *Geostand. Newslett.* 19, 1–23.
- Woodhead, J.D., Hergt, J.M., 2005. Preliminary appraisal of seven natural zircon reference materials for in situ Hf isotope determination. *Geostand. Geoanal. Res.* 29, 183–195.
- Woodhead, J., Hergt, J., Shelley, M., Eiggins, S., Kemp, R., 2004. Zircon Hf-isotope analysis with an excimer laser, depth profiling ablation of complex geometries, and concomitant age estimation. *Chem. Geol.* 209, 121–135.
- Yılmaz, O., Bonhomme, M.G., 1991. K-Ar isotopic age evidence for a lower to middle Jurassic low-pressure and a lower Cretaceous high-pressure metamorphic events in north-central Turkey. *Terra Abstr.* 3, 501.
- Yılmaz, Y., Tüysüz, O., 1984. Kastamonu-Boyabat-Vezirköprü-Tosya arasındaki bölgenin jeolojisi (İlgaz-Kargı masiflerinin etüdi). MTA rapor No. 7838. (in Turkish).
- Yılmaz, O., 1980. Daday-Devrakani masifi kuzeydoğu kesimi lithostratigrafi birimleri ve tektoniği. *Yerbilimleri* 5–6, 101–135 (in Turkish).
- Yılmaz, O., 1983. Çangal metafilyonun mineralojik-petrografik incelenmesi ve metamorfizma koşulları. *Yerbilimleri* 10, 45–58 (in Turkish).